Reply on the Reviewers' comments on the paper

"A satellite-derived database for stand-replacing windthrow events in boreal forests of European Russia in 1986–2017"

(essd-2020-91)

Andrey Shikhov, Alexander Chernokulsky, Igor Azhigov, Anastasia Semakina

We would like to thank two anonymous reviewers and Dr. Barry Gardiner for their valuable and constructive comments on our manuscript. Following the suggestions of reviewers, we made a revision of the manuscript including clarifying some aspects of the data collection process, correction of grammar and syntax errors, implementation of minor revisions. In particular, we have renamed sections, added a new figure. We have uploaded the new version of the dataset with changed objects numbering and with the readme file that describes the structure of attribute tables and the units. Because of language correction, we have changed the title of the manuscript to 'A satellite-derived database for stand-replacing windthrow events in boreal forests of European Russia in 1986–2017'.

The point–to–point answers on reviewers' comments are listed below.

Anonymous Referee #1:

The manuscript "A satellite-derived database for stand-replacing windthrows in boreal forests of the European Russia in 1986–2017" present a GIS-database on storm events in European Russia. The data base spans more than 30 years and contains over 100,000 entries, an enormous amount of data! As such, I believe that the manuscript and database are an important addition to the literature, as information on windthrows is rare. I applaud the authors for undertaking such a great effort in compiling the data. That said, I have some issues and comments, which in my opinion need to be addressed before publication.

(1) The assessment includes a lot of subjective calls from the interpreter and there is no formal validation. I fully understand that validating the database is very challenging, but I would have at least expected some assessment on how accurate the data is. There are many steps involved in collecting the data, and some of them seem to be highly dependent on local knowledge. From this I assume that the accuracy will be higher in some regions (where there is ample local knowledge), but lower in others. In particular, I was wondering whether you searched the forest area of ER systematically or whether you applied any other "sampling strategy" to ensure you don't miss a storm event. Moreover, the accuracy will depend on the availability of HRI. Was HRI available for each year after 2001, or only for selected years? The authors address some of these issues in the discussion, which I appreciated, but maybe they should make clear from the beginning on that the database is a subjective collection and probably far from complete and/or consistent.

We agree that due to several limitations of the method and satellite data the database is spatially and temporally inhomogeneous and hence incomplete. We have added corresponding information into the Abstract. Sections 2, 4, and 6 were also amended.

We devoted the whole Section 6 to discussing of factors influencing the data accuracy including such factors as percentage of forest-covered area, forests species composition and forest management practices. In general, our data has highest accuracy for low-populated northern and eastern part of the ER, where forests cover 70-90% of the territory and dark-coniferous forests are widespread. In turn, the data may be less accurate for southern part of the study area, where some windthrow areas probably could be missed. The relevant information has been added to Section 6.

Each windthrow from our dataset was validated (that is, it was clarified that it is actually a windthrow), based on pre- and post-event Landsat/Sentinel-2 images, high-resolution images and additional information. So, the probability that any forest disturbance was mistakenly referred to a windthrow is minimal. However, we agree with the reviewer, that some thresholds used in the data collection process, in particular the thresholds for the minimum area of EDAs and windthrow, as well as the threshold for the minimum distance for separating successive windthrow, are somewhat subjective.

We should stress, that the searching of windthrow areas based on GFC/EEFCC was systematic. The GFC/EEFCC-based collection of forest loss areas with windthrow-like signatures was carried out separately for each region of the ER. A grid with 50 km cell size was built inside the region, which helped to organize the searching of windthrow-like forest disturbances. The relevant information has been added to Section 4.1.1.

The HRI are available only for several years (usually 2-8 images for the entire period 2001-2017), and the year of 2001 is the only year of the appearance for the first HRI. Wherein, some areas in the northern part of the ER are not covered by HRI. However, the lack of HRI affects determination of windthrow type (windstorm- or tornado-induced) rather its identification accuracy. The relevant information has been added to Section 2.2.

(2) In the same line as the previous comment, many of the decision to group patches to windthrows, etc. are based on arbitrary thresholds. I wonder whether the authors have tested the sensitivity of their results to those thresholds. The allocation of patches to windthrow events might look very different with slight changes in threshold values.

Indeed, in our method, we used a number of thresholds that have some subjectivity but are based on previous studies. For instance, the 10-km threshold for separate successive windthrow from each other is based on study of Doswell and Burgess (1988), who proposed the 5–10 miles (8–16 km) threshold for the gap to separate one skipping tornado from two successive tornadoes. The threshold for minimum area of EDAs was chosen based on study of Koroleva and Ershov (2012) who showed high uncertainty of estimated geometrical characteristics of small-scale windthrow (less than 1800 m^2, i.e., two GFC pixels). In addition, we decided to filter out such small-scale disturbances since it is virtually impossible to confirm their wind-related origin.

We performed sensitivity test for the latter threshold and found that the absence of minimum accepted area for EDAs will increase area of windthrow by 2-3% on average (up to 6%). The optimization of other threshold values can be evaluated in further studies that should involves ground-based data.

We have added this information to Sections 4.1.1 and 4.1.4.

(3) You do not explain how the Landsat data was processes. Please give some details on the processing.

We downloaded Landsat images (L1T processing level) from https://earthexplorer.usgs.gov/ and https://eos.com/landviewer. We did not use any atmospheric correction algorithm for the image preprocessing (see our rationale below). For NDII-based delineation process, we used only images with cloudiness less than 10% based on CFMask algorithm (Foga et al., 2017). For other purposes (verification, type and date determination), we visually inspected Landsat images for lacking clouds over the area of interest (i.e., a windthrow area).

The relevant description been added to the revised version of the manuscript (to different parts of Section 4). The reference 'Foga et al., 2017' has been added to the reference list.

Moreover, how many Landsat images were available per year, on average?

The availability of cloudless Landsat images varied from year to year. The lowest number of cloud-free images (2-4 images a year on average) is available for 2003-2006 and 2012, when only Landsat-7 (SLC-off) data were available (Potapov et al., 2015). Hence, the worst accuracy of windthrow date determination is typical for these years.

On average, 8-10 cloud-free images per year can be used for windthrow identification and dates determination. Due to Sentinel-2A satellite launching, number of images per year had an abrupt increase after the summer of 2016.

We have added this information to Section 4.4.

I guess that in Russia many winter images are covered by snow. As you use pre/post windthrow Landsat images to ensure windthrow detection, data availability is crucial. In years with only few observations, detection accuracy might be lower.

Winter images (of land covered with snow) were successfully used for windthrow identification, especially if a storm occurred at the end of summer season, and autumn season lacked cloud-free images.

(4) The manuscript is already well written, but needs some language editing. I give some suggestions below. Also, it is quite dry to read in some parts, but I guess this is typical for a data paper.

We thank the reviewer for his suggestions on language editing.

Specific comments:

Throughout the manuscript: No "the" needed before "European Russia".

Corrected (including the title).

L. 17: Sentence starting with "Additional. . .": Something wrong with the sentence, please revise (e.g., "Additional information, such as . . ., is also provided."

Corrected.

L. 21: Change to ". . ., which is in contrast to . . .".

Corrected.

L. 23: Change to ". . . can be used by both science and management."

Corrected.

L. 28: "Forests are. . ."

Corrected.

L. 29: "Exposed to. . ." and replace "and windstorms" to "or windstorms".

Corrected.

L. 37: ". . ., and droughts. . ."

Corrected.

L. 38: Remove "the" before "Western. . ."

Corrected.

L. 41: Change to ". . .like increasing growing stock. . ."

Corrected.

L. 43: Remove "as well".

Corrected.

L. 46: Remove "of" before "wind-related . . ."

Corrected.

L. 56: Remove "substantially"

Corrected.

L. 62: Replace "on the Earth" with "globally"

Corrected.

L. 66: Replace "publication" with "opening"

Corrected.

L. 75: Replace "the archive of Landsat images" with "the Landsat archive"

Corrected.

L. 76: Remove "the" before "public map. . ."

Corrected.

L. 79: Add "the" before "windthrow delineation. . ."

Corrected.

L. 74-82: You rather describe where you do what in the manuscript, which is not of interest at this point. I strongly suggest to revise this paragraph to give a detailed description of what data and which specific attributes you will collect; and what is the rational for collecting those.

Corrected. The paragraph has been partially rewritten; the description of the data and specific attributes has been added. The sentence on the importance of collecting the windthrow database has been added to the previous paragraph.

L. 88: "study region" not "study regions". It is also not clear to me what the following sentence means. Please revise.

Corrected, the second part of the sentence has been removed.

L. 93: What is "the large area"? Do you mean a specific area?

Corrected.

L. 100ff: Why is this written in bullet points? I strongly suggest to write the section out as proper text.

Corrected.

L. 101/102: Change to ". . . forest disturbance at annual temporal resolution."

Corrected.

L. 108: Change to ". . . on forest loss classified into. . ."

Corrected.

L. 122: How do you download images from Google Maps or Bing Maps?

The sentence has been completely rewritten.

L. 175: This might be a personal flavor, but could you give the areas in hectare or square meters? A value of 0.0018 km2 is hard to image, given all the leading zeros.

Corrected.

Section 4.1.1.: How did you ensure you didn't miss a windthrow? Was there some systematic sampling design applied? How can you be sure there are only 450 windthrows? Did you look any each and every disturbance patch?

We assume that the searching of windthrow areas based on GFC/EEFCC was rather systematic. The GFC/EEFCC-based collection of forest loss areas with windthrow-like signatures was carried out separately for each region of the Russian Federation. A grid with 50 km cell size was built inside each region, which helped to organize the searching of windthrow-like forest disturbances — the searching was performed sequentially in each cell of the grid. However, we agree, that some windthrow areas can be missed and discuss it in Section 6. Moreover, since we used the threshold values of windthrow area (0.05 km^2 for tornado-induced windthrow areas and 0.25 km^2 for other windthrow), all forest disturbances with smaller area are missed in our database. The relevant information has been added to Section 4.1.1.

L. 195: Revise beginning of the sentence.

Corrected.

L. 200: How was the Landsat data processed? Were any corrections or masking algorithms applied? More information needed.

We applied none atmospheric correction algorithm for preprocessing Landsat images, since NDII is based on the near-infrared (0.76 - 0.90 nm) and middle-infrared (1.55 - 1.75 nm) spectral bands that are almost insensitive to atmospheric impact. We used images with cloudiness less than 10% based on CFMask algorithm (Foga et al., 2017). The relevant information has been added to the text.

L. 211: Change "the stand-replacing" to "a stand-replacing"

Corrected.

L. 212: Not sure what is meant by "However, this value may be less if these disturbances hold the substantial part of the image."? Please explain.

The paragraph has been rewritten for clarity.

We estimated threshold value from the statistics of ΔNDII raster. Firstly, we obtained the mean value and standard deviation of ΔNDII within the entire forest-covered area on image. Stand-replacing forest disturbance inherently has ΔNDII values substantially higher than the image average. To separate stand-replacing forest disturbance from other forest-covered area, we used the threshold value of two standard deviations, which was previously tested by Koroleva and Ershov (2012). However, in some cases the ΔNDII distribution within the entire image was skewed (e.g., due to the presence of cloud decks or haze on the post-event image). In such cases, we lowered the threshold value of ΔNDII iteratively by comparing the detected changes with results of visual identification of windthrow on a post-event image (using several examples located in different parts of windthrow). As a result, actual threshold values ranged from 1.5 to 2 standard deviations. Then, a binary raster of detected changes (i.e., forest losses) has been created (see fig. 4d) and converted to a shapefile. This information has been added to Section 4.1.3.

L. 230: "A similar threshold value. . ."

Corrected.

L. 230ff: Here for instance I have the feeling that the choice of thresholds is very subjective and depends largely on the interpreter and his/her knowledge. How can we make sure that the data collection is systematic and not biased?

We selected this threshold values based on Doswell and Burgess (1988), who proposed the 5-10 miles (8-16 km threshold for the gap length to separate one skipping tornado from two successive tornadoes. It is also important, that this threshold determines only geometrical characteristics of single windthrow (the second layer of the GIS database) and do not affect the total area of a storm event (the third layer of the GIS database). The relevant text has been added to Sections 4.1.4 and 4.3.

L. 270: How did you assess whether a storm happened in winter? My guess is that satellite data and HRI data is mostly only available for the growing period.

The availability of the Landsat and Sentinel-2 images does not depend on the season of a year, excluding some years, e.g. 2003–2006, when only the Landsat-7 (SLC-off) images were available. In fact, wintertime images were widely used at all stages of the data collection. We agree with the reviewer that the frequency of obtaining of cloudless images in autumn and winter was lower than in summer season, but it was sufficient for the analysis. The text in Section 4.4 has been corrected to highlight this issue.

L. 292ff: How was the central line drawn? By hand? Or did you use an algorithm to do so? Is the line sensitive to the allocation of patches to wind throw events?

The central line was created automatically (using a Python tool) as a distance between two farthest points of a windthrow. It is insensitive to the allocation of patches to windthrow area. The explanation has been added to Section 4.3.

L. 389ff: This is discussion and not results. In genera you mix up a lot of results reporting and discussion. In general, I think that is fine for such a paper, but then you should rename the section to Results and Discussion; and give the Discussion section a more informed title.

We agree. The section "Results" has been renamed to "Results and Discussion", and the section "Discussion" has been renamed to "Data and method limitations"

L. 446: You note that no winter windthrows were found. This might be a result of missing winter observations, right?

Both Landsat-based products GFC and EEFCC reveals stand-replacing windthrow area regardless of the season of its appearance. In particular, if windthrow happened in winter it would be clearly seen on image taken in subsequent vegetation period because of rather slow forest recovery process. Therefore, the revealed lack of winter windthrow is feasible due to the climatic conditions of the study area and does not associated with data limitations. In particular, winter storms from Western Europe reach the territory of Russia already weakened (Haylock, 2011), while low temperatures and soil freezing also prevent stand-replacing windthrow in Russian forests during winter season (Suvanto et al., 2016). According to (Suvanto et al., 2016), winter windthrow are not typical for Finland as well. The relevant information has been added to Section 5.3.

Conclusion section: You are cautious in interpreting trends in windthrow area due to inconsistencies in your data. This is great and much appreciated. However, you then conclude that the positive trend for large windthrows likely is "real". But how do you come to this conclusion? Without proper validation, we can't be sure about this. I suggest to remove this conclusion.

We agree with this suggestion and have removed this conclusion.

Comments on the database:

The dataset was downloadable and could be opened in standard GIS software (QGIS).All entries had attributes. The projection of the GIS layers was set. Units were not specific. I thus encourage the authors to add a README or similar metadata file to describe the units (i.e., are, length, etc.).

We agree. The 'Readme' file that describes the structure of attribute tables and the units has been added to the dataset. We have also changed the objects numbering inside each GIS layer of the database (the relevant description has been added to Section 3). The URL address of the dataset has been changed to https://doi.org/10.6084/m9.figshare.12073278.v6

Anonymous Referee #2:

The manuscript described the development of a satellite-driven GIS database containing information on stand-replacing windthrows in boreal forests of the European Russia between 1986 and 2017. Based on this database the spatial and temporal distribution of windthrows in European Russia is also presented in the manuscript. The manuscript is well structured and written (although the large number of acronyms make the reading difficult in places) and is free of errors in logic. Furthermore, the manuscript is filling a gap concerning the climatology of severe storms in European Russia, especially in the sparsely populated area.

Minor comments

line 10: "natural disturbances" is not clearly defined in this context

The word “natural” has been deleted.

line 14: "[...] determine the type of"

Corrected.

line 17: "[...] with an area"

Corrected.

line 18: replace "contained" with "containing"

Corrected according to the suggestion of the first reviewer. The phrase has been modified as follows: “Additional information such as weather station reports and event description from media sources is also provided”.

line 21: "[...] happened in the summer"

Corrected.

line 24: no need to include this information in the abstract.

We agree; the information has been removed.

line 29: from my point of view "disturbance" is not a good choice of word in this context

‘Natural disturbance agent’ is a commonly used term relating to wildfires, windstorms, insect outbreaks, etc. (see e.g. Ulanova, 2000; Seidl et al., 2017).

line 36: "Particularly, both the [...]"

Corrected.

line 45: "[...] convective storms in the warm season"

Corrected.

line 50: not sure what "macro-regional" is in this context

The word ‘macro-regional’ is has been replaced by ‘international’.

line 52: replace "presented" with "compiled"

Corrected.

line 54: remove extra open parenthesis

Corrected.

line 100: "[...] that occurred"

Corrected.

lines 151-155: maybe the authors should add a figure containing examples of the "three hierarchical levels"

A new figure 3 has been added that shows an example with all three hierarchical levels of the database, explains the determination of geometric characteristics of storm event, and shows the examples of parallel and successive windthrow. Correspondingly, numbers of all subsequent figures have been changed.

line 208-210: the choice of thresholds is not clearly defined

The paragraph has been rewritten for clarity.

We estimated threshold value from the statistics of ΔNDII raster. Firstly, we obtained the mean value and standard deviation of ΔNDII within the entire forest-covered area on image. Stand-replacing forest disturbance inherently has ΔNDII values substantially higher than the image average. To separate stand-replacing forest disturbance from other forest-covered area, we used the threshold value of two standard deviations, which was previously tested by Koroleva and Ershov (2012). However, in some cases the ΔNDII distribution within the entire image was skewed (e.g., due to the presence of cloud decks or haze on the post-event image). In such cases, we lowered the threshold value of ΔNDII iteratively by comparing the detected changes with results of visual identification of windthrow on a post-event image (using several examples located in different parts of windthrow). As a result, actual threshold values ranged from 1.5 to 2 standard deviations. Then, a binary raster of detected changes (i.e., forest losses) has been created (see fig. 4d) and converted to a shapefile. This information has been added to Section 4.1.3.

lines 220-240: is not clear how the thresholds used in this section have been derived

We used the 10-km threshold as the slightly modified value proposed by Doswell and Burgess (1988) who suggested to use the 5–10 miles (8–16 km) threshold for a gap to discriminate between one skipping tornado and two successive tornadoes. The reference to (Doswell and Burgess, 1988) has been added to the revised version of the manuscript.

line 261: the ratio of length to width of 10:1 is based on previous studies conducted for European Russia?

Yes. This is typical ratio for tornado length and width for US (Schaefer and Edwards, 1999) and for Northern Eurasia (Shikhov and Chernokulsky, 2018).

The clarification has been added to the revised version of the manuscript.

line 323: "[...] we calculated as well"

Corrected.

line 323: "estimation" instead of "estimating"

Corrected.

line 348: citation not in the correct form

We have checked the correctness of the citation.

line 361: citation not in the correct form

We have checked the correctness of the citation.

line 439: "storm events occurred"

Corrected.

line 472: is not clear what the authors meant by "contain fewer plots"

A typical tornado-induced windthrow event on average contains less EDAs than non-tornado induced one. The word “Plots” has been replaced by “EDAs”.

Interactive comment from Barry Gardiner

Main Points

1. Language needs some help. I would recommend the paper being checked by a native English paper because in some places the meaning was not totally clear.

Language has been improved.

2. Unlike the earlier reviewer I was really impressed at how much effort was put into assessing the potential errors in the assessment. I also think the authors were completely honest about limitations in the data and their assessments. Such honesty will give really help users of the data.

In the revised version, we made minor changes according to the first reviewer suggestions.

Minor Points

1. I would recommend referencing the paper Ulanova, N.G., 2000. The effects of windthrow on forests at different spatial scales: a review. For. Ecol. Manage.135, 155–167. https://doi.org/10.1016/S0378-1127(00)00307-8 This paper deals with the effects of wind in the Russian boreal forest. It is a brilliant and seminal paper.

The reference to this paper has been added in the Introduction section.

2."windthrow" not "windthrows" throughout. Plurals in English can be difficult.

Corrected (including the title).

3. I think early on you need to tell the reader that your analysis was done manually and not automated. That is important to understand the process. Also refer whenever possible to Fig. 2 which is super useful.

We have added the word ‘manually’ into the Abstract. Additionally, the short sentence on the manual character of the data analysis has been added to the beginning of Section 4. The additional references to figure 2 have been added throughout the text.

4. Page 6. I think some more justification of the limits you set would be helpful, for example the lower limits on size of EDAs.

We removed all EDAs with an area ≤ 1800 m^2 that equals to area of two GFC pixels. We filtered out such small-scale disturbances since it is virtually impossible to confirm their wind-related origin. Moreover, the area of local windthrow can be almost three times overestimated by Landsat images (Koroleva and Ershov, 2012). Thus, this is the balance between slight underestimation of the total area of windthrow (by 2-3%) in the study region and substantial overestimation of the number of EDAs mistakenly referred to windthrow. We have decided to choose the first option.

We have added this rationale to Section 4.1.1.

5. Page 7. What did you do in highly populated areas? Did you just accept that you will have missed wind damage on some occasions?

Indeed, the windthrow data obtained for the period before 2000 (using the EEFCC dataset) may be incomplete for highly-populated regions of the ER due to assignment of forest losses to broad periods, i.e., 1986–1988 and 1989–2000. To partially avoid missing of windthrows, using Landsat images, we performed additional verification of all large-scale forest loss areas (with area more than 5 km^2) in these regions independently of their geometry, since windthrow areas

can be totally masked out by logged areas. Thus, we were able to find three large-scale windthrow events in highly-populated regions of the ER. However, some windthrow events can still be missed.

The clarification has been added to Section 4.1.2.

6. Page 7, line 212. Use "represent" not "hold".

The paragraph has been completely rewritten according to the suggestions of the first reviewer.

7. Page 8, line 222. Again justify the figure of 5-10 km. Do you use "rules" or is this judgement left to the observer?

We used the 10 km threshold, which is in the range of 8–16 km (5–10 miles) proposed by Doswell and Burgess (1988) to discriminate between one skipping tornado and two successive tornadoes. Therefore, if the nearest EDAs were located at a distance more than 10 km from each other, they belonged to different windthrow. If the distance between them was less or equal to 10 km, they belong to one windthrow except for several cases. The exceptions were associated with changes of windthrow direction, transformations of one windthrow type to another identified by the HRI, and abrupt change of forest damage degree.

8. Page 9, line 261. I think "predominately" is better than "prevalently".

Corrected.

9. Page 11, line 346. I think the symbol should be ~ rather than <

Corrected.

10. Page 13, line 367. When you say "less than 13%" what are you referring to? 13% of what?

It is less than 13% of the total area of windthrow events. Corrected.

11. Page 13, line 392. But trees could break. You don't manage wind break at all in your paper.

It is of note, that we cannot determine whether the trees were felled or broken by the wind based on satellite images, even having very high resolution. Therefore, we use a single term "windthrow" for all types of wind-induced forest damage.

This clarification has been added to the beginning of Section 5.

12. Page 13, line 398. Please define "parallel" and "successive".

Successive windthrow areas induced by one storm event follow downwind one after another and approximately fall on one straight line (the angle of deviation from this line does not exceed 10-20°). Such windthrow are presumably induced by one convective cell generating a sequence of squalls or tornadoes. In contrast, parallel windthrow areas that located within one storm event are situated parallel to each other (with an angle less than 30°). They are presumably associated with two or more different convective cells or mesocyclones, generating squalls or tornadoes, often embedded into one mesoscale convective system. The examples of parallel and successive windthrow are shown at new Fig. 3.

The definitions have been added to Section 4.1.4.

13. Page 14, line 417. What do you mean by dark-coniferous? What species are you referring to?

Dark-coniferous forests in the ER consist of three dominating tree species such as Picea abies, Picea obovata and Ábies sibírica. We have added this information to section 2.1.

14. Page 14, line 430. Too coarse for what? Correlation? With what?

The sentence has been deleted. Instead, we highlighted, that using out dataset, estimates of relationship between windthrow area and forest stands characteristics can be carried out in future studies at a regional scale.

15. Page 15, line 461. Write out local time not LT.

Corrected.

16. Page 490. Reference work in USA and Amazon on damage from derechos or squall lines. See a) Negrón-Juárez, R.I., Chambers, J.Q., Guimaraes, G., Zeng, H., Raupp, C.F.M., Marra, D.M., Ribeiro, G.H.P.M., Saatchi, S.S., Nelson, B.W., Higuchi, N., 2010. Widespread Amazon forest tree mortality from a single cross-basin squall line event. Geophys. Res. Lett. 37, 1–5. https://doi.org/10.1029/2010GL043733 and b) Peterson, C. J., 2000: Catastrophic wind damage to North American forests and the potential impact of climate change. Sci. Total Environ.,262, 287–311.

Both references have been added.

References:

Doswell, C.A. and Burgess, D.W.: On some issues of United States tornado climatology. Monthly Weather Review, 116, 495–501, 1988.

Foga, S., Scaramuzza, P.L., Guo, S., Zhu, Z., Dilley, R.D., Beckmann, T., Schmidt, G.L., Dwyer, J.L., Hughes, M.J., and Laue, B. Cloud detection algorithm comparison and validation for operational Landsat data products. Remote Sensing of Environment, 194, 379-390. http://doi.org/10.1016/j.rse.2017.03.026, 2017

Haylock, M, R.: European extra-tropical storm damage risk from a multi-model ensemble of dynamically-downscaled global climate models. Natural Hazards and Earth System Sciences, 11, 2847–2857, doi:10.5194/nhess-11-2847-2011, 2011.

Koroleva, N. V., and Ershov, D. V.: Estimation of error in determining the forest windfall disturbances area on high spatial resolution space images of LANDSAT-TM. In: Current Problems in Remote Sensing of the Earth From Space, 9, 80–86, 2012. (in Russian)

Schaefer, J.T., and Edwards, R., The SPC tornado/severe thunderstorm database. In: Preprints, 11th Conf. on Applied Climatology. Amer. Meteor. Soc, Dallas, TX Available online at. https://ams.confex.com/ams/99annual/abstracts/1360.htm (6.11), 1999.

Seidl, R., Thom, D., Kautz, M., Martin-Benito, D., Peltoniemi, M., Vacchiano, G., Wild, J., Ascoli, D., Petr, M., Honkaniemi, J., Lexer,, M.J., Trotsiuk, V., Mairota, P., Svoboda, M., Fabrika, M., Nagel T.A. and Reyer, C. P. O.: Forest disturbances under climate change, Nature Climate Change, 7(6), 395–402. doi:10.1038/nclim ate33 03, 2017.

Suvanto, S., Henttonen, H. M., Nöjd, P., and Mäkinen, H.: Forest susceptibility to storm damage is affected by similar factors regardless of storm type: Comparison of thunder storms and autumn extra-tropical cyclones in Finland, Forest Ecology and Management, 381, 17–28, doi: 10.1016/j.foreco.2016.09.005, 2016.

Ulanova, N.G.: The effects of windthrow on forests at different spatial scales: a review. Forest Ecology and Management 135, 155–167. doi:10.1016/S0378-1127(00)00307-8, 2000.

A satellite-derived database for stand-replacing ~~windthrows~~windthrow events in boreal forests of ~~the European Russia~~European Russia in 1986–2017

Andrey N. Shikhov[1], Alexander V. Chernokulsky[2], Igor O. Azhigov[1] and Anastasia V. Semakina[1]

[1]Perm State University, Perm, 614990, Russia
[2]A.M. Obukhov Institute of Atmospheric Physics, Russian Academy of Sciences, Moscow, 119017, Russia

Correspondence to: Andrey N. Shikhov (shikhovan@gmail.com)

Abstract. Severe winds are among the main causes of ~~natural~~ disturbance~~s~~ in boreal and temperate forests. Here, we present a new GIS database of stand-replacing ~~windthrows~~windthrow events in the forest zone of ~~the European Russia~~European Russia (ER) for the 1986–2017 period. Delineation of ~~windthrows~~windthrow areas was based on the full Landsat archive ~~of Landsat images~~ and two Landsat-derived products on forest cover change, namely the Global Forest Change and the Eastern' Europe Forest Cover Change datasets. Subsequent verification and analysis of each windthrow was carried out manually to determine ~~a~~ the type of related storm event, its date or date range, and geometrical characteristics. The database contains 102,747 elementary areas of damaged forest that were combined into 700 ~~windthrows~~windthrow ~~areas~~events caused by 486 convective or non-convective storms. The database includes stand-replacing ~~windthrows~~windthrow only, ~~which~~ with an area > 0.05 km^2~~5 ha~~ and > 0.25 km^2 ~~25 ha~~ for events caused by tornadoes and other storms, respectively. Additional information such as ~~contained~~ weather station reports and event description from media sources is also provided. The total area of stand-replacing windthrow amounts to 2966 km^2, that is 0.19% of the forested area of the study region. Convective windstorms contribute 82.5% to total wind-damaged area, while tornadoes and non-convective windstorms are responsible for 12.9% and 4.6% of this area, respectively. Most of ~~windthrows~~windthrow events in ~~the ER~~ER happened in ~~to~~ the summer, which ~~that~~ is in contrast to Western and Central Europe, where ~~windthrows~~~~windthrow~~they mainly occur in autumn and winter. Due to ~~numerous~~several data and method limitations, ~~of the data sources and the use of expert knowledge at several stages of the data collection workflow,~~the compiled database is~~f probably far from complete~~spatially and temporally inhomogeneous and hence incomplete. But despite this incompleteness, the ~~compiled~~presented database provides a valuable source of spatial and temporal information on windthrow in ER and can be used by both science and management. ~~The compiled database provides a valuable source of spatial and temporal information on windthrows~~windthrow ~~in the ER~~ER ~~and can be used by both science and management~~can be successfully used both in forest science and severe storm studies. The database is available at https://doi.org/10.6084/m9.figshare.12073278.v3 ~~(Shikhov et al., 2020).~~

1 Introduction

Forests are ~~is~~ a valuable natural resource that is important for economy, society and sustainable development. Forest~~s~~ ecosystems are regularly exposed ~~by~~ to natural disturbance agents such as fires, droughts, insect outbreaks, ~~and~~ or windstorms. Being an intrinsic part of forest ecosystem dynamics (Attiwill, 1994; Seidl et al., 2017), natural disturbance~~s~~s~~s~~ cause substantial environmental and economic damage (Schelhaas et al., 2003; Gardiner et al., 2010; van Lierop et al., 2015). In boreal and temperate forests, windstorms constitute~~s~~ one of the main drivers of natural disturbance~~s~~s~~s~~ (Ulanova, 2000; Forzieri et al., ~~2019~~2020). In Europe, ~~windthrows~~windthrow contribute more than a half to the total area of natural disturbance~~s~~s~~s~~, including abiotic and biotic causes (Schelhaas, 2003; Gardiner et al., 2010).

Recently, disturbance regimes have changed considerably in many forest ecosystems worldwide (Seidl et al., 2011, 2017; Senf et al., 2018). Particularly, both the occurrence and severity of disturbance~~s~~ ~~both~~ has increased in different regions, including those related to forest fires (Westerling, 2016; Kukavskaya et al., 2016), insect outbreaks (Kautz et al., 2017), and droughts (Millar et al., 2015). Researchers have revealed a statistically significant increase of wind-related forest disturbance~~s~~ in ~~the~~ Western, Central, and Northern Europe (Seidl et al., 2014; Gregow et al., 2017), and in ~~the~~ European ~~part of~~ Russia (Potapov et al., 2015).

The observed increase in the frequency and severity of ~~windthrows~~windthrow events is associated with changes in forest structure ~~like~~ like increasing growing stock ~~a rise of growing stock~~ and median age, primarily in coniferous forests (Schelhaas et al., 2003; Senf et al., 2018), and with climatic changes ~~as well~~ (Overpeck et al., 1990; Lassig and Moĉalov, 2000; Seidl et al., 2011; 2014; 2017). An intensification of winter windstorms (Gardiner et al., 2010; Usbeck et al., 2010; Gregow et al., 2017) and an increase in the frequency and intensity of severe convective storms in ~~a~~ the warm season (Overpeck et al., 1994; Diffenbaugh et al., 2013; Chernokulsky et al., 2017; Radler et al., 2019) can be considered as the main climatic drivers for increasing ~~of~~ wind-related damage in boreal and temperate forests.

For correct attribution of forest ~~windthrows~~windthrow to particular causes, it is important to obtain corresponding data on such events. Recently, several long-term databases of ~~windthrows~~windthrow events in boreal and temperate forests, often together with other types of disturbance~~s~~, have been collected at a national and ~~macro-regional~~international scale. The longest ~~windthrows~~windthrow data series have been compiled in Sweden (Nilsson et al., 2003) and Switzerland (Usbeck et al., 2010) based on literature reviews and forestry services reports. European Forest Institute ~~presented~~ compiled the database of destructive storms in European forests for 1951−2010 (Gardiner et al., 2010). A new GIS database of wind disturbance~~s~~ in European forests has been compiled in 2019 by aggregating multiple datasets collected by 26 research institutes and forestry services across Europe (Forzieri et al, ~~(2019~~2020). It comprises more than 80.000 forest areas that were disturbed by wind in 2000-2018. Compare to other European countries, ~~windthrows~~windthrow events in Russia remain ~~substantially~~ understudied. Long-term databases of ~~windthrows~~windthrow events have been collected only for individual

regions, for example, for the Middle Ural (Lassig and Moĉalov, 2000) and the Central Forest Reserve in the Tver' region (Ulanova, 2000).

The main data sources of exist windthrow databases in Russia were the literature reviews, reports of forestry services, aerial observations and field investigations (Skvortsova et al., 1983; Lassig and Moĉalov, 2000; Ulanova, 2000). Meanwhile, satellite images have become the important data source for windthrowswindthrow monitoring in Russian forests in recent decades (Krylov et al., 2012). Indeed, satellite data can be especially informative for studying Russian low-populated boreal forests, known in Russia as the taiga, which represent the largest forested region globallyon the Earth. They cover approximately 7.63 million km^2, which is 22% of the world's forest areas (WWF Russia's boreal forests, 2007).

Use of satellite images for obtaining information on windthrow was proposed back in 1975 (Sayn-Wittgenstein and Wightman, 1975). However, the widespread utilising of satellite data to estimate the inter-annual variability of windthrowswindthrowwind-related forest damage (e.g. Fraser et al., 2005; Baumann et al., 2014) became feasible after the openingpublication of the free-available Landsat archive (Wulder et al., 2012), and two Landsat-based products, namely the Global Forest Change (GFC) map (Hansen et al., 2013) and the Eastern' Europe Forest Cover Change (EEFCC) (Potapov et al., 2015). Thus, GIS databases of windthrowswindthrow events have been collected for some Russian regions based on Landsat archive and GFC data, i.e., for the Ural and north-eastern part of the ERER (Shikhov and Zaripov, 2018; Shikhov et al., 2019), Kostroma region and adjacent areas (Petukhov and Nemchinova, 2014), and South Sakhalin (Korznikov et al., 2019). Shikhov and Chernokulsky (2018) found 110 previously unknown tornado-induced windthrowswindthrow areas in the ERER based on satellite images. However, for the entire ER, there are only rough estimates of storm-related forest damage (Potapov et al., 2015). The contribution of various weather phenomena like (convective and non-convective windstorms, snowstorms, or and tornadoes) to the total wind-induced forest damage, geometrical characteristics of windthjrows and alsoas well as inter-annual and seasonal distribution of windthrow events remains unknown for the territory of ER. SuchThe appearance of such data can be helpful both for forest science and management andas well as for severe storms investigations.

In this study, we present a detailed GIS database of relatively large and stand-replacing windthrow events in the forest zone of the the ERER for the period 1986-2017. UnlikeThe database contains the above-described studies, this database will contain the stand-replacing windthrow areas with indication of storm event types and dates, geometrical characteristics of windthrows areas, and additional information. To compile the data and determine theirthese attributescharacteristics, Wwe use the Landsat archivethe archive of Landsat images, the Landsat-based forest loss data products GFC and EEFCC, high-resolution satellite images from the public map services, supplementary information including weather stations observations, databases on hazardous weather events, damage reports in the media sources, and reanalysis data. We describe the used data and the study region in section Section 2, and explain the database structure in Section 3. Section 4 describes the windthrow delineation process and assessment of the geometrical parameters of windthrowswindthrow areas. Section 5 presents spatio-temporal variability of windthrowswindthrowwind-damaged areas and distributions of their geometrical characteristics.

Section ~~5~~ 6 discusses the main limitations of the method and the compiled dataset, while Section 6 draws the main conclusions of the paper.

2 Region and data

2.1 The study region

The study region includes the forest zone of the ~~the ER~~ER (Fig. 1) between the forest-steppe transition zone on the south and forest-tundra transition zone on the north. The availability of the EEFCC dataset determines the eastern boundary of the study region that broadly coincides with the Ural Ridge.

We used the 250-m resolution map of the vegetation cover of Russia (Bartalev et al., 2016) to estimate forest-covered area and dominant forest species (Fig. 1). Forests cover 54.6% of the study region~~s, while individual forested area within this region is typically > 100 km^2~~. The most widespread dominant forest species are dark-coniferous (*Picea abies, Picea obovata, ~~Pinus sylvestris~~Ábies sibírica*), light-coniferous (*Pinus sylvestris*), small-leaved (*Betula pendula, Betula pubescens, Pópulus trémula*) and some broadleaved species (*Tília cordáta, Quercus robur et al.*) (Kalyakin et al., 2004). Secondary (re-grown after logging or wildfires) small-leaved and mixed forests cover approximately 61% of the total forested area. Old-growth dark-coniferous forests are widespread on the western slope of the Northern Ural and the adjacent plain, and pine forests cover the largest area (>100 thousand~~.~~ km^2) on the northwest of the ~~the ER~~ER (Fig. 1).

2.2 Initial data

We used multiple data sources to collect information on ~~windthrows~~windthrow events for the 1986-2017 period. Particularly, we utilized satellite data to delineate ~~windthrows~~windthrow areas and determine a storm event type and used additional information to determine the dates of storm events.

Primary information for windthrow delineation and verification

The Landsat-based GFC data were utilised to search and delineate ~~windthrows~~windthrow ~~that occurred~~~~the~~forest areas affected by wind~~throw~~ in 2001–2017. The data come as the integer raster with a 30 m cell size. It contains information on stand-replacing forest disturbances at annual temporal resolution~~forest disturbances that classified with a one year step~~. In the boreal forest regions, the overall accuracy of the forest loss detection in the GFC is 99.3%, while user's and producer's accuracies are 93.9% and 88.0%, respectively (Hansen et al., 2013). Here, producer's accuracy is the ratio of correctly classified forest loss area to the actual forest loss area; user's accuracy is the ratio of correctly classified forest loss area to the same area according to the verified forest loss area. The data were downloaded from http://earthenginepartners.appspot.com/google.com/gMG7KbLG.

The EEFCC dataset was used to search and delineate ~~windthrows~~windthrow ~~the~~ areas ~~affected by windthrow occurred~~ in 1986–2000. The data come as the integer raster with a 30 m cell size. It contains information on forest loss ~~that~~ classified into four broad periods: 1986-1988, 1989-2000, 2001-2006 and 2007-2012. This rough time determination is associated with

rareness of the Landsat images between 1989 and 1998. The detection of gross forest loss in the EEFCC has producer's and user's accuracy of 88% and 89%, respectively (Potapov et al., 2015). The data were downloaded from https://glad.geog.umd.edu/dataset/eastern-europe-forset-cover-dynamics-1985-2012/.

Landsat images (L1T processing level), i.e., images from the Landsat Thematic Mapper (TM), Enhanced Thematic Mapper Plus (ETM+), and Operational Land Imager (OLI), were used to confirm the wind-related nature of forest disturbances, determine the storm types, dates (or ranges of dates) of ~~windthrows~~windthrow occurrence in 1986–2017. It addition, many ~~windthrows~~windthrow areas appeared ~~occurred~~ before 2001 were delineated with Landsat images (see Section 3.1.3 for details).

Sentinel-2 images were used to confirm the wind-related nature of forest disturbances, determine the storm types, dates (or ranges of dates) of ~~windthrows~~windthrow events occurrence for the 2016–2017 period. ~~The data were~~We downloaded Landsat and Sentinel-2 images from https://earthexplorer.usgs.gov/ and https://eos.com/landviewer.

High-resolution (0.5–2 m) satellite images, hereinafter HRI, were used to discriminate the type of a storm event — windstorm or tornado — causing ~~a~~ windthrow. ~~The HRI are available for several years from 2001 to the present (u~~Usually 2–8 high-resolution images are available for the ~~entire~~ period 2001–2017~~)~~. No HRI are available before 2001. To view and analyze HRI, we used mainly Google Earth Pro, while other ~~The HRI images were downloaded obtained from Google Earth Pro and~~ public map services ~~(~~, i.e., ~~Google Maps,~~ Bing Maps, ESRI Imagery, ~~and~~ Here~~)~~, were used to a lesser degree~~ESRI Imagery, and Google Earth Pro~~. We should highlight that t~~T~~he availability of HRI substantially vary~~ied for~~among different parts of ER. ~~Thus~~In particular, some areas in the northern part of the ER are not covered by HRI.

Additional information on storm events

Information of 3-hourly weather reports was used to determine storm event dates, and match the reported wind gusts, if any, with ~~windthrows~~windthrow events. We utilized information on observed wind speed, precipitation, hail and thunderstorm occurrence. The routine meteorological observations have been collected at 402 meteorological stations located within the studied area and have been initially processed at the All-Russian Research Institute of Hydrometeorological Information—World Data Center (RIHMI-WDC) from 1966 to the present (Bulygina et al., 2014).

Monthly reviews of hazardous weather events occurred in Russia, which are published in the Russian Meteorology and Hydrology journal (http://mig-journal.ru/en/archive-eng) but not translated, were also used to determine storm event dates for the 2001–2017 period. Additionally, these reviews contain the descriptions of hazardous weather events and damage reports. We included this information into our database.

The RIHMI-WDC database of hazardous weather events (Shamin et al., 2019) and information from regional departments of the Russian state weather service were also utilized to determine the dates of several storms that caused ~~windthrows~~windthrow events in 1986–2017.

Media news and witness reports in social networks, including photos and videos, were used for obtaining additional information on the type of event, i.e., tornadic or non-tornadic, for the 1986–2017 period.

Data from meteorological satellites Terra/Aqua MODIS (from 2001) and Meteosat-8 (from 2016) were used for obtaining additional information on storm events causing windthrow, especially to determine storm date and time. In particular, the Collection 6 MODIS Active Fire data (Giglio et al., 2016) were used to discriminate fire- and wind-related forest disturbances in 2001–2017. Data were downloaded from https://earthdata.nasa.gov/data/near-real-time-data/firms.

Data from Russian weather radars (Dyaduchenko et al., 2014) were used only for several events occurred in 2012, 2014, and 2016 to determine the time of storm event causing a windthrow.

3 Structure of the GIS database

The compiled database of stand-replacing windthrowswindthrow events in the forest zone of the ERER in 1986-2017 is publicly available at https://doi.org/10.6084/m9.figshare.12073278.v3https://doi.org/10.6084/m9.figshare.12073278.v36 (Shikhov et al., 2020). We divided the spatial and attributive information on windthrowswindthrow events into three hierarchical levels that correspond to three GIS layers, i.e., three shapefiles (.shp), in the database:

- "Elementary damaged area" (EDA), that is a single-part polygon of wind-damaged forest;
- "Windthrow", that represent a group of closely spaced forest disturbances, i.e., a multipart polygon, associated with one storm event;
- "Storm event track", that is a cluster of windthrowswindthrow areas with having identical similar direction and having the same date (or same date range) of occurrence, which were most likely induced by one convective or non-convective storm.

GIS layers have WGS84 geographic coordinate system (EPSG:4326). The key fields *ID* and *storm_ID* associates each damaged area with the spatial features in the datasets of windthrowswindthrow and storm event tracks respectively using one-to-many relation. ID values of windthrow areas are set according to the date of occurrence of storm events. Within one year, numbers are first set for windthrow areas with known dates, and then for ones with unknown dates. If two or more windthrow areas are caused by one storm event, their numbers are sequential according to storm movement directionly. The numbering of EDAs is organized according to the numbering of windthrow areas. EDAs related to one windthrow area are numbered from the lower left corner, that is, from southwest to northeast. The structure of the attribute tables of each shapefile (stored in .dbf files) is presented at Tables 1–3. The determination process of the presented characteristics is described in Section 4 and schematically presented at Fig. 2. Figure 3 shows an example with all three hierarchical levels of the database.

4. Methods: windthrow delineation and parameters determination

The process of ~~windthrows~~windthrow identification and attribution to a particular type includes four stages (Fig.2): (1) delineation of a windthrow using the Landsat-based GFS and EEFCC products or time series of Landsat or Sentinel satellite images, (2) subsequent verification of a windthrow using the HRI and determination of the type of a storm event causing a windthrow, (3) estimation of geometrical characteristics of a windthrow, and (4) determination of storm date or range of dates by utilizing additional information. Most of data collection stages were performed manually using standard GIS tools, except for the data extraction from the GFC and EEFCC products and calculation of ~~windthrows~~ the geometrical characteristics of windthrow areas (that were automated with Python language). Due to ~~numerous~~several limitations of the data sources and the use of expert knowledge at ~~several~~different stages of the data collection workflow (Fig. 2), the compiled database is spatially and temporally inhomogeneous and hence incomplete~~if probably far from complete~~. In particular, the database lacks small-scale forest disturbances with area below thresholds (Fig. 2). The main data and method limitations ~~of the data collection workflow~~ are discussed in ~~the~~ Section 6.

4.1 Delineation of windthrow areas

4.1.1 GFC-based delineation (2001-2017)

We systematically searched through the GFC dataset for forest loss areas that have characteristic windthrow-like signatures. ~~The searching of windthrow areas based on GFC was rather systematic.~~ The ~~GFC-based collection of forest loss areas with windthrow-like signatures~~search was ~~carried out separately~~performed for each ~~region~~cell of a supplemental ~~of the Russian Federation. A~~ grid with 50 km cell size that was built ~~inside each region~~for the ER~~, which helped to organize the searching of windthrow-like forest disturbances – the searching was performed sequentially in each cell of the grid~~. ~~(the searching was performed sequentially in each cell of the grid)~~ ~~However, it is highly likely that some windthrow areas were missed (see Section 6 for more details). Since we used the threshold values of windthrow area (0.05 km^2 for tornado-induced windthrow areas and 0.25 km^2 for other windthrow), we did not estimate the forest disturbance with a smaller area. The relevant information has been added to the section 4.1.1.~~

In particular, we looked for ~~windthrows~~windthrow the forest disturbances with the shape ~~that~~ ~~elongated~~ stretched along the direction of storm or tornado movement. Wind-related forest disturbance~~s~~ rarely have quasi-circular/elliptic or regular shapes that are characteristic for fire-related disturbance~~s~~ and logged areas, respectively (Shikhov and Chernokulsky, 2018, Shikhov et al., 2019). Windstorm- or snow/icestorm-caused ~~windthrows~~windthrow areas have amorphous spatial structure and a varying degree of forest damage, whereas tornado-induced ~~windthrows~~windthrow areas have quasi-linear spatial structure and almost total removal of a canopy (Chernokulsky and Shikhov, 2018). After selecting an area affected by a windthrow, we extracted respective pixels from the GFC data and converted them from raster to multipart vector polygons, which consist of many singlepart polygons, so-called ‘elementary damaged area~~s~~’ (EDA~~s~~, fig. 2, fig. 3~~6~~). ~~In addition, we~~

~~removed all EDAs with an area ≤ 0.0018~~1800 ~~km~~^{2}~~, that is two GFC pixels.~~ We removed all EDAs with an area ≤ 1800 m^2 ~~t~~that equals to area of two GFC pixels. We filtered out such small-scale disturbance since it is virtually impossible to confirm their wind-related origin. Moreover, the area of local windthrow can be almost three times overestimated by Landsat images (Koroleva and Ershov, 2012). We found, that the absence of minimum accepted area for EDAs will increase area of windthrow by 2-3% on average (up to 6% for several windthrow areas with amorphous spatial structure). However, the number of EDAs mistakenly referred to windthrow can be substantially overestimated. ~~Thus, the use of minimum accepted area for EDAs is the balance between slight underestimation of total area of windthrow in the study region and substantial overestimation of the number of EDAs mistakenly referred to windthrow. We have decided to choose the first option. The optimization of other threshold values can be evaluated in further studies that should involves ground-based data.~~

~~We filtered out such small-scale disturbances since it is~~ often ~~impossible to confirm their wind-related origin. Moreover, their area of local windthrows can be almost three times overestimated by Landsat images (Koroleva and Ershov, 2012). By removing small-scale EDAs, we can slightly underestimate the area of windthrow in general, but the number of EDAs mistakenly referred to windthrow substantially reduced.~~

In total, we delineated 450 ~~windthrows~~windthrow areas using the GFC dataset, and clarified contours of 126 of them manually using the Landsat, Sentinel-2, or HRI images (see Section 4.2 for details).

4.1.2 EEFCC-based delineation (1986–2000)

For the EEFCC data, we performed similarly to the GFC searching and delineation of ~~windthrows~~windthrow areas with however some limitations. The main limitation is related to the classification of forest losses into broad periods, i.e., 1986-1988 and 1989-2000. Thereby, windthrow area can be correctly delineated only if it lacks overlap with other forest disturbance~~s~~, namely loggings and wildfires, occurred in the same period. For instance, in high~~l~~y-populated areas, salvage loggings are usually performed in 1–2 years for most of wind-damaged forests. Such ~~windthrows~~windthrow areas were delineated by the Landsat images with semi-automated NDII-based method (see Section 4.1.3). Based on the EEFCC, we were able to delineate ~~windthrows~~windthrow areas with high confidence mainly in the low-populated northern part of the ~~the ER~~ER (Fig. 4~~3~~). To partially avoid missing of windthrow areas, using Landsat images, we performed additional verification of all large-scale forest loss areas (with area more than 5 km^2) in highly-populated regions independently of their geometry, since windthrow areas can be totally masked out by logged areas. We were able to find three large-scale windthrow events (≥ 10 km^2) in these regions. However, some windthrow events can still be missed.

~~To avoid missing large-scale windthrow in highly-populated areas, we additionally verified in such regions all large-scale forest disturbances (with an area ≥ 5 km^2, that is not typical for industrial logging in the forest zone of ER). These forest loss areas were verified by multi-temporal Landsat images independently of their geometry, since windthrow areas can be totally masked out by logged areas. Thus, we were able to find three large-scale (≥ 10 km2) windthrow areas in highly-populated regions of ER. However, some windthrow event can be missed.~~

In total, we delineated 153 ~~windthrows~~windthrow areas using the EEFCC dataset. Contours of the 32% of them were then substantially clarified manually with the Landsat images, obtained before and after the storm events. Another 22 ~~windthrows~~windthrow areas that occurred before 2001 were delineated manually using the Landsat images. As for the GFC, we removed all EDAs with an area < ~~0.0018 k~~1800 m^2, since it is often impossible to confirm their wind-related origin.

4.1.3 NDII-based delineation (1987-2000)

We used Landsat TM/ETM+ images (Level 1T) obtained before and after the storm event in the growing season to delineate seven~~7 In total, seven~~ large-scale ~~windthrows~~windthrow, occurred before 2001~~, were delineated by comparing Landsat TM/ETM+ images obtained before and after the storm event in the growing season~~. We used the difference of Normalized Difference Infrared Index (NDII, Hardisky et al., 1983) to detect and delineate wind-related disturbance~~s~~. High efficiency of the NDII using for ~~windthrows~~windthrow identification on Landsat images has been shown previously (Wang et al., 2010; Wang and Xu, 2010; Chernokulsky and Shikhov, ~~1984~~2018). NDII was formulated as follows:

$$NDII = (TM4 - TM5)/(TM4 + TM5), \quad (1)$$

where TM4 and TM5 are the reflectance in the bands 4 (0.85 μm) and 5 (1.65 μm) of Landsat TM/ETM+ data, while the difference was calculate as $\Delta NDII = NDII_{before} - NDII_{after}$, where subscripts 'before' and 'after' denotes two closest to an event cloud-free images obtained, respectively, before and after the windthrow occurrence, but in the growing season only.

We applied none atmospheric correction algorithm for preprocessing Landsat images, since NDII is based on the near-infrared (0.76 - 0.90 nm) and middle-infrared (1.55 - 1.75 nm) spectral bands that are almost insensitive to atmospheric impact. ~~the near-infrared (0.76 - 0.90 nm) and middle-infrared (1.55 - 1.75 nm) spectral bands that are less sensitive to atmospheric influences in comparison to visible spectrum bands.~~ For NDII-based delineation process, we used only images with cloudiness less than 10% based on CFMask algorithm (Foga et al., 2017). For other purposes (verification, type and date determination), we visually inspected Landsat images for lacking clouds over the area of interest (i.e., a windthrow area)~~Cloud masking was also not required since we used thousands of images, and most of them were needed only to determine the dates of previously delineated windthrow. In its turn, the images that were used for windthrow delineation were cloudless within the area of interest.~~

The masking of forested lands was performed on the 'before' image with the use of Iterative Self-Organizing Data Analysis Technique Algorithm (Ball and Hall, 1965) unsupervised classification. Then, the NDII was calculated only within the mask of the forested area. The same technique was successfully applied previously to delineate ~~windthrows~~windthrow areas caused by the 1984 Ivanovo tornado outbreak (Chernokulsky and Shikhov, ~~1984~~2018).

~~Windthrows~~Windthrow and other forest disturbance~~ss~~ are characterized by a sharp decrease of the NDII. However, threshold values of ΔNDII for distinguishing between stand-replacing disturbance~~s~~ and moderate damaged or undamaged forest~~s~~, differ for each pair of images. We estimated threshold value from the statistics of ΔNDII raster. Firstly, we obtained the mean value and standard deviation of ΔNDII within the entire forest-covered area on image. Stand-replacing forest

disturbance inherently has ΔNDII values substantially higher than the image average. To separate stand-replacing forest disturbance from other forest-covered area, we used the threshold value of two standard deviations, which was previously tested by Koroleva and Ershov (2012). However, in some cases the ΔNDII distribution within the entire image was skewed (e.g., due to the presence of cloud decks ~~iness decks~~ or haze on the post-event image). In such cases, we lowered the threshold value of ΔNDII iteratively by comparing the detected changes with results of visual identification of windthrow on a post-event image (using several examples located in different parts of windthrow). As a result, actual threshold values ranged from 1.5 to 2 standard deviations. Then, a binary raster of detected changes (i.e., forest losses) has been created (see fig. 5~~4~~d) and converted to a shapefile.~~We estimated threshold value from the statistics of ΔNDII raster. Firstly, we obtained the mean value and standard deviation of ΔNDII within forest-covered area. Stand-replacing forest disturbance has ΔNDII values substantially higher than the average for the image. To separate stand-replacing forest disturbance from other forest-covered area, we used threshold value of two standard deviations, which was previously tested by Koroleva and Ershov (2012). However, in some cases the ΔNDII distribution for the entire image was asymmetric (e.g. due to the presence of cloudiness on the post-event image), In such cases, we corrected threshold value manually, to ensure the best fit with the results of the visual identification of windthrow. In most cases, the pixels with values of ΔNDII that exceed the average value for the forested areas of the entire image by more than two standard deviations, indicate the stand-replacing forest disturbances (Koroleva and Ershov, 2012). However, this value may be less if these disturbances hold the substantial part of the image. We estimated the threshold values from a sample of ΔNDII, obtained within the forested area, and corrected it in several cases to ensure the best fit with the results of the visual identification of windthrows. The threshold values ranged from 1.5 to 2 standard deviations for different pair of images.~~ ~~On~~ At the next step, ~~windthrows~~windthrow areas were separated from logged areas and other disturbance~~s~~ (see Section 3.2). The EDAs ≤ ~~0.0018 k~~1800 m^2 were removed. Figure ~~4~~ 5 presents the example of the NDII-based identification of the aftermath on 21 June 1998 Moscow windstorm (Los Angeles Times, 1998).

4.1.4 Combining delineated polygons to a windthrow areas and ~~windthrows~~windthrow areas to a storm event tracks

In general, a group of closely spaced EDAs, caused by one storm event, was assigned to one windthrow. By the 'close distance' we meant in most cases a distance of tens or hundreds of meters between the nearest EDAs. This distance is determined manually by the proportion of stand-replacing damage ~~(the distance decrease as its increasing)~~, and the presence of treeless areas. Maximum distance between nearest EDAs combined to one windthrow area ~~However, it~~ may reach ~~5~~ 10 km, if a windthrow crossed treeless areas ~~(fig. 7 may be an example)~~.

Most of ~~windthrows~~windthrow areas were extracted from the GFC dataset (450 ~~windthrows~~windthrow), EEFCC dataset (153 ~~windthrows~~windthrow) or with NDII-based methods (7 ~~windthrows~~windthrow). ~~For t~~These ~~windthrows~~windthrow areas were~~,~~ ~~we~~ first automatically delineated ~~a gross outline of a windthrow~~ as a multi-part polygons, and then we specified exact contours of ~~its~~ their components — single-part polygons (EDAs)~~;~~. ~~a~~After that, we correctly merged them to a windthrow itself (F~~f~~ig. 2). We delineated other 90 ~~windthrows~~windthrow areas manually using the Landsat, Sentinel-2, or

HRI images — 30, 17, and 43 ~~windthrows~~windthrow areas, respectively. In this case, we first delineated EDAs and then merged them into a windthrow.

Many storms induced a series of successive ~~windthrows~~windthrow areas, which are separated from each other by tens or even hundreds of kilometres of undamaged forests, treeless areas or water bodies (F~~f~~ig. ~~6~~3). In general, we divided the damaged areas into two separate ~~windthrows~~windthrow (two records in the dataset), if the gap between them exceeded 10 km. ~~The~~ This threshold is based on the study of Doswell and Burgess (1988), who proposed the 5–10 miles (8–16 km) threshold for the gap to ~~separate~~discriminate between one skipping tornado ~~from~~and two successive tornadoes. ~~A similar threshold value (8 km) was previously used proposed to separate one skipping tornado from two successive tornadoes (Doswell and Burgess, 1988; Shikhov and Chernokulsky, 2018).~~ A few exceptions were associated with changes of windthrow direction, transformations of one windthrow type to another identified by the HRI, i.e., the tornado-induced to non-tornado-induced, and with abrupt change of forest damage degree — from 60–~~-~~80% to 5–~~-~~10% of stand-replacing disturbance~~s~~. In these cases, the distance between two distinct ~~windthrows~~windthrow areas was less — for instance, the minimum distance was about 1 km when a tornado-induced windthrow transformed to a squall-induced one.

If several ~~successive or quasi parallel~~close ~~windthrows~~windthrow areas have similar direction, differing by no more than 30°, and the same date (or date range) of occurrence, we assigned them to one storm event ~~(fig. 6)~~. We highlight successive and parallel windthrow areas (Fig. 3). Successive windthrow areas induced by one storm event follow downwind one after another and approximately fall on one straight line (the angle of deviation from this line does not exceed 10-20°). Such windthrow are presumably induced by one convective cell generating a sequence of squalls or tornadoes. In contrast, parallel windthrow areas that located within one storm event are situated parallel to each other (with an angle less than 30°). They are presumably associated with two or more different convective cells or mesocyclones, generating squalls or tornadoes, often embedded into one mesoscale convective system. ~~Successive windthrow areas follow downwind one after another and approximately fall at one straight line (the angle of deviation from this line does not exceed 10-20°). Such windthrow are presumably induced by one convective cell generating a sequence of squalls or tornadoes. In contrast, parallel windthrow are located parallel to each other or at a large angle (over 45°). They are presumably associated with two or more different convective cells or mesocyclones, generating squalls or tornadoes, often embedded into one mesoscale convective system.~~

The expert-based process of windthrow areas combining to a storm event was based as well on various additional information including the storm dates and types (see next sections), information from weather station reports, eye-witness and newspaper reports, data from meteorological satellites, and so on. ~~Threshold value of a distance between different windthrow areas related to one storm event was not determined, and maximum distance between them reaches 150 km.~~ In total, the dataset of storm event tracks contains 486 items.

~~The threshold values used in this section (maximum distance to combine EDAs to windthrow area and minimum distance to separate two successive windthrow areas) have some subjectivity, and their modification may substantially change the number of allocated windthrow areas in the dataset. However, these thresholds determine only length and width of single~~

~~windthrow, and they does not affect the total area of windthrow, which is the main characteristic of wind induced forest disturbances. The optimization of above-described threshold values can be considered as a further research direction.~~

360

4.2 Verification of ~~windthrows~~windthrow events and determination of its type

At the second stage, we ~~performed expert based verification for each forest disturbance~~verified each windthrow area in the database using pre- and post-event Landsat/Sentinel-2 images, high-resolution images and additional information~~the HRI or, in the lack of the HRI, the Landsat/Sentinel-2 images~~. This verification was performed to ensure the forest disturbance was
365 caused by wind and to determine a type of a storm caused a windthrow. In total, we verified 54% of ~~windthrows~~windthrow areas with the HRI, mainly for the 2001-2015 period. Other ~~windthrows~~~~windthrow~~events were verified using the Landsat images (22% of ~~windthrows~~windthrow), the Sentinel-2 images (9%) and additional data sources like weather station and eye-witness reports (15%). As a result, the probability that any forest disturbance was mistakenly referred to ~~a~~ windthrow is minimal.

370 In addition, we used the last cloud-free Landsat or Sentinel-2 image obtained before a storm and first image obtained after to separate ~~windthrows~~windthrow areas from other disturbance~~s~~, mainly from logged areas. We removed forest disturbance~~s~~ that were not related to a storm event (Fig. 6~~5~~). During the verification, we also found and delineated several storm-damaged areas that were missed in the GFC/EEFCC data. Such areas are located mainly in small-leaved or broadleaved forests. After the verification, we determined the type of a windthrow depending on a weather phenomenon induced this windthrow. We
375 selected tornado-induced and non-tornado-induced ~~windthrows~~windthrow areas, the latter were subdivided into induced by convective and by non-convective storms. In turn, non-convective storms include also snowstorms, which are indicated in the database but not analyzed separately further in the paper. By convective storms we mean squalls and downbursts; however, this more detailed division lacks in the database.

To distinguish tornado-induced ~~windthrows~~windthrow areas from other wind-related disturbance~~s~~, we determined the
380 direction of fallen trees using the HRI. Indeed, the main signature of tornado-induced ~~windthrows~~windthrow is the counterclockwise, or infrequently clockwise, rotation of the fallen trees (Beck and Dotzek, 2010; Shikhov and Chernokulsky, 2018). In the lack of the HRI, we considered three additional signatures of tornado-induced ~~windthrows~~windthrow, namely (1) quasi-linear structure of a windthrow with a ratio of length and width ≥ 10:1, (2) a gradual turn of a storm track, and (3) predominately~~prevalently~~ total removal of forest stands (Shikhov and Chernokulsky,
385 2018; Shikhov et al., 2019). Note, that the ratio of length and width of tornado track ≥ 10:1 is also typical for U.S. (Schaefer and Edwards, 1999). Based on these three signatures and additional information from weather station reports, witness reports, photos and videos, we assigned the high or medium degree of certainty of storm type determination for each windthrow (Table 4).

~~Windthrows~~Windthrow areas, caused by non-convective windstorms or snowstorms, have as well specific geometrical
390 features that seen at satellite images. Specifically, ~~windthrows~~windthrow areas related to non-convective windstorms typically have enormous length and width of the damage track, up to 200 and 45 km respectively, with however slightly or

moderate damaged forests. ~~Caused by non-convective windstorms s~~Stand-replacing disturbance~~s~~ caused by non-convective windstorms are usually occur in dark coniferous forests only (Dobbertin et al., 2002; Schmoeckel and Kottmeier, 2008). Since non-convective storms affect large areas and last for relatively long period, they are typically well-reported by weather stations, which simplify the attribution of related ~~windthrows~~windthrow. In its turn, snowstorm-induced ~~windthrows~~windthrow areas are distinguishable from other disturbance~~s~~ primarily based on the dates of occurrence — they happen usually in autumn; although, one severe snowstorm occurred in early summer. It is of note, that we found none of snowstorm-induced stand-replacing windthrow happen in winter.

After the determining of a storm event type, we excluded from the database the tornado-induced ~~windthrows~~windthrow with an area ≤ 0.05 km^2 and non-tornado-induced ~~windthrows~~windthrow with an area ≤ 0.25 km^2. We took into account the following reasons during exclusion of such small-scale ~~windthrows~~windthrow areas:

1. Difficulty to prove that these disturbances ~~are~~ were actually ~~were~~ caused by wind, especially in the lack of the HRI.
2. Difficulty to determine ~~wind~~ storm event dates with the Landsat images for these ~~windthrows~~windthrow areas.
3. High uncertainty of estimated geometrical characteristics of small-scale ~~windthrows~~windthrow (Koroleva and Ershov, 2012; Shikhov and Chernokulsky, 2018).

Only five squall-induced ~~windthrows~~windthrow with an area < 0.25 km^2 were stored in the database, since they are associated with severe weather outbreaks with proven dates. It is of note, that a typical tornado-induced windthrow consist of a relatively small number of EDAs with total removal of forest stands that are well-detected by the Landsat images. In its turn, a typical non-tornado-induced windthrow include larger number of small-scale (i.e., 2-4 Landsat pixels) areas of stand-replacing disturbances, that are worse detected by satellite images. This difference results in the necessity of using two distinct thresholds for tornado- and non-tornado-induced ~~windthrows~~windthrow areas.

The threshold values used in Sections 4.1–4.2 have some subjectivity, and their modification may substantially change the number of allocated windthrow areas in the dataset. The optimization of above-described threshold values can be evaluated in further studies that should involves ground-based data.

4.3 Estimation of geometrical parameters of ~~windthrows~~windthrow areas and storm tracks and its accuracy

We used Landsat data and the Landsat-based products GFC and EEFCC to estimate geometrical parameters of ~~windthrows~~windthrow areas. We determined the path length (L), mean and maximum widths (W_{mean} and W_{max}), and damaged area (A) for each windthrow using the technique that had been successfully implemented for tornado-induced ~~windthrows~~windthrow areas (Shikhov and ~~,~~ Chernokulsky, 2018). The calculation of these parameters was performed in the Lambert Equal Area and Equidistant projection for North Asia to avoid possible projection-related distortions.

We calculated A in the ArcGIS 10.4 as the sum of area of forest damaged plots, which are attributed to one windthrow. We determined L as a length of the central line drawn through a damaged area, i.e. distance between two farthest points of a

windthrow. The central line was created automatically (using a Python tool) as a distance between two farthest points of a windthrow. It is insensitive to the allocation of patches to windthrow area.

We calculated W_{mean} as the mean length of several transects that are perpendicular to a storm track with a 200 m step; this step had been found optimal in terms of quality and counting efficiency (Shikhov and, Chernokulsky, 2018). Only stand-replacing ~~windthrows~~windthrow areas were taken into account in this calculation. In comparison to (Shikhov and, Chernokulsky, 2018), where W_{max} were calculated manually using the HRI data, in this study, we assigned the length of the largest transect to W_{max} because the lack of the HRI for many ~~windthrows~~windthrow areas.

In addition to windthrow characteristics, we estimated geometric characteristics of EDAs and those of storm tracks. Particularly, for EDAs, we calculated their area A_{EDA}. For storm tracks, we estimated maximum and mean width (W_{TRmean} and W_{TRmax}), path length (L_{TR}), and damaged area (A_{TR}). We calculated W_{TRmean} based on the same transects that were used to calculate W_{mean} but without excluding undamaged forests and treeless areas. Similarly, length of the largest transect that includes undamaged forests and treeless areas was assigned to W_{TRmax} (Fig. ~~6~~7). If a track consists of two (or more) parallel ~~windthrows~~windthrow areas, then its width was calculated within the outermost boundaries of these ~~windthrows~~windthrow areas (Fig. 3). The same calculation was performed for L_{TR} in case of two (or more) subsequent ~~windthrows~~windthrow areas (Fig. 3). Thus, the used 10-km threshold (see Section 4.1.4) may influence geometrical characteristics of single windthrow area, but do not affect those of a storm event.

We assessed the accuracy of GFC-based estimates of windthrow geometrical parameters by comparing them with the same parameters calculated manually with the use of HRI ~~using~~. We performed such procedure for ten ~~windthrows~~windthrow areas caused by squalls, whose area ranges from 0.26 to 6.09 km^2 (Table 5). Distribution of their A is close to the one for the full dataset.

We delineated manually all EDAs within these ten ~~windthrows~~windthrow areas using the HRI. In total, we found 837 and 947 EDAs, according to the GFC and the HRI data respectively. Owing to relatively correct georeference of the Landsat data (Landsat Collection 1, 2019), we found no systematic spatial bias between contours of GFC-based and HRI-based ~~windthrows~~windthrow areas. Despite their general matching, there is no complete overlap due to different spatial resolution of the GFS and HRI (Fig. ~~7~~8). For example, one GFC-based EDA may intersect with several HRI-based ones, and vice versa. We found, that only 66.5% of the total area is attributed to ~~windthrows~~windthrow in both GFC and HRI, while EDAs with small area can be missed. In particular, 263 HRI-based EDAs with the total area of 0.97 km^2 were completely missed in the GFC, while 146 GFC-based EDAs with the total area of 0.52 km^2 were missed in the HRI. For overlapped EDAs, we found the mean absolute error and root mean square error of A_{EDA} estimates amounted to 27.6% and 13.1%, respectively. We found that the relative error decreases for large EDAs and for those having a simple shape, i.e., quasi-circular. The user's and producer's accuracies increase from 20–25% for EDAs with A_{EDA} < 0.01 km^2 to 70–75% for EDAs with A_{EDA} > 0.1 km^2. In general, for the overlapped EDAs, the GFC overestimates their A_{EDA} (by 4% on average) primarily in coniferous forests. Mutual effect of more frequent omission of small EDAs in the GFC compare to the HRI and overestimation of overlapped

EDAs results in approximate equality of total area of delineated ~~windthrows~~windthrow — 17.11 km^2 and 17.13 km^2 based on the GFC and HRI, respectively.

For entire ~~windthrows~~windthrow area, we ~~as well~~ calculated as well an accuracy of their geometrical characteristics ~~estimating~~estimate~~sion~~. In particular, we calculated the user's and producer's accuracies of the GFC-based delineation for each of ten selected windthrow. These accuracies are mainly determined by the complexity of windthrow shapes and composition. In particular, the accuracy is higher for a windthrow consisting of relatively small number of simple-shape EDAs. Otherwise, the accuracy decreases down to 50% for a windthrow ~~with is~~having ~~-~~very amorphous spatial structure. In our sample, the GFC data tends to overestimate the area of ~~windthrows~~windthrow — eight cases out of ten were overestimated. The mean absolute percent error (MAPE) for A is 14.6%. The major overestimation of A by the GFC data, as well as W_{mean} and W_{max}, was revealed for relatively small ~~windthrows~~windthrow areas. This is in line with the previous findings by Koroleva and Ershov (2012). They ~~who~~ showed that the reliable estimate (with 15% accuracy) of the damaged area using the Landsat images is possible only for ~~windthrows~~windthrow areas exceeding 0.026 km^2. It is of note, that for tornado-induced ~~windthrows~~windthrow areas, Shikhov and Chernokulsky (2018) found, that the GFC data generally tends to underestimate A, with MAPE amounted to 17.9%.

The assessment of geometrical parameters of ~~windthrows~~windthrow areas appeared ~~occurred~~ before 2000 and found by the EEFCC is challenging due to the low availability of the HRI or other independent data sources, e.g. the data of forestry services. ~~Windthrows~~Windthrow areas induced by storm events that occurred >20 years ago can be delineated by the HRI only if a~~they~~ storm passed through old-growth forests that have not been affected by other disturbance~~s~~, i.e., timber harvesting or wildfires, in subsequent years. Such forests are widespread only in the northeastern part of the ~~the ER~~ER (Pakhuchiy, 1997). We found five EEFCC-based ~~windthrows~~windthrow appeared occurred between 1998 and 2000 that were most well-detected by the HRI — four tornado-induced and one non-tornado induced. We delineated them with the EEFCC and the HRI and compare their characteristics (Table 6). We found general overestimation of A, W_{mean} and W_{max} in the EEFCC, that was larger than in the GFC. It may be related to the inclusion into a windthrow not only real wind-damaged pixels but also surrounding pixels where tree had died after a windthrow appearance mostly because of bark beetles (Köster et al., 2009). Intensity of this mortality is highest at a second year after a storm event (Köster et al., 2009).

4.4 Determination of windthrow dates

We aimed to establish the exact date or even the exact time for each windthrow appearance. However, due to data constraints, dates of some ~~windthrows~~windthrow events were determined with ~~accuracy ≃<~~ 6 months accuracy. We iteratively refined date, or a date range, by using different data. The process, related to the determination of date of tornado-induced ~~windthrows~~windthrow only, had been described previously in (Shikhov and Chernokulsky, 2018).

First, the year of a windthrow can be obtained directly from the Landsat products but with some limitations. In the GFC, forest disturbance~~s~~ are accompanied with information on the year of event occurrence. However, the exact year is determined correctly only for 75.2% of ~~events~~forest loss pixels; for ~~21~~24.~~58~~% of ~~events~~them, the date can be either ~~a~~ 1 ~~-~~2

year earlier or ~~a year~~ later (Hansen et al., 2013). In the EEFCC, a year of windthrow occurrence is not explicitly determined and came within the ranges 1986–1988 and 1989–2000 years.

Next, we refined a range of dates based on all available images from the Landsat and Sentinel-2 satellites. The accuracy of such refinements depends on a frequency of observations and cloudiness. The availability of cloudless Landsat images varied from year to year~~strongly fluctuated from year to year~~. The lowest number of cloud-free images (2–~~–~~4 images a year on average) is available for 2003–~~–~~2006 and 2012, when only Landsat-7 (SLC-off) data are available (Potapov et al., 2015). Hence, the worst accuracy of windthrow date determination is typical for these years. ~~The lowest frequency of satellite observations in the study area, namely 2–4 cloud-free images per year, took place in 2003–2006, 2008, and 2012 years when only Landsat-7 data were available (Potapov et al., 2015).~~ On average, 8-10 images per year can be used for windthrow ~~identification and~~ dates determination. ~~In turn,~~ Due to Sentinel-2A satellite launching, number of images per year had an abrupt increase after the summer of 2016~~t~~The highest frequency of satellite imagery, namely ten images per month for a location, was achieved in 2016–2017 after the start of the Sentinel-2 mission~~.~~ We used images taken throughout a year.

Despite the frequency of cloudless images in autumn and winter was lower than in summer season, it was sufficient for analysis. Thus, ~~It is of note also that~~ winter images (of land covered with snow) were successfully used for windthrow identification, especially if a storm occurred at the end of summer season, and autumn season lacked cloud-free images. ~~wintertime images (of landobtained when land surface is covered with snow) were widely used for windthrow identification, especially if a storm occurred at the end of summer season, and autumn season lackedwas without cloud-free images. The frequency of obtaining of cloudless images in autumn and winter was lower than in summer season, but is it is sufficient for analysis, especially considering that we used all images cloud-free over the area of interest (i.e. over a windthrow area).~~

Further, given the satellite-derived range of event possible dates, we made the subsequent analysis using additional data such as weather station observations, various databases and reviews on hazardous weather events, damage reports, photos and videos in the media and social networks, and reanalysis data (see (Shikhov and ~~and~~ Chernokulsky, 2018) for details). This analysis allowed to establish the exact dates for 48.4% of all ~~windthrows~~windthrow events including 39.2% and 59.7% of tornado- and non-tornado-induced ~~windthrows~~windthrow events, respectively.

The dates of storm-induced ~~windthrows~~windthrow events were defined more successful than those for tornado-induced ~~windthrows~~windthrow~~ones~~ due to the local nature of convective storms, especially of tornadoes, and a relatively large distance between Russian weather stations. Specifically, the average and median distance between nearest weather stations within the study area amounted to 53.7 and 49.9 km, respectively. Wherein, many storm events were reported by weather stations located on a storm path at a distance of 50-100 km from a windthrow, while the closest stations did not reported strong wind gusts since they were away from a storm path. In total, we matched storm reports of weather stations, namely reports with wind gusts ranges from 15 m/s to 34 m/s, only with 34.5% of ~~windthrows~~windthrow events with known date.

Another reason for more successful determination of dates of appearance for large-scale ~~windthrows~~windthrow areas than for small-scale ~~windthrows~~windthrow~~ones~~, e.g., tornado-induced, is an increase of probability that a corresponding storm

passes through a settlement(s) and this is covered in the media. In total, we used media reports, information from regional weather services, witness photos and videos, existed scientific literature (e.g., Dmitrieva and Peskov, 2013; Petukhov and Nemchinova, 2014; Shikhov and Chernokulsky, 2018; Shikhov et al., 2019) to specify the date and time of 29.7% of ~~windthrows~~windthrow events.

Dates and time of some cases (7.8% of all cases) were established using images from meteorological satellites Terra/Aqua MODIS and METEOSAT-8, and Russian weather radar data (Dyaduchenko et al. 2014). However, the routine usage of these data is time-consuming and limited due to some access restrictions. Subsequent clarification of windthrow exact time can be carried out in further studies.

5 Results and discussion

5.1 Windthrow type

The compiled database includes three shapefiles (.shp), corresponding to three hierarchical levels such as elementary damaged areas, ~~windthrows~~windthrow, and storm events. The database includes 102747, 700, and 486 objects for each level, respectively ~~(fig. 2)~~. The total area of the spatial features is equal 2966.1 km^2. It is of note, that we cannot determine whether the trees were felled or broken by the wind based on satellite images, even having very high resolution. Therefore, we use a single term "windthrow" for all types of wind-induced forest damage.

The overwhelming majority of found stand-replacing ~~windthrows~~windthrow in ~~the ER~~ER, namely 97.4% of ~~windthrows~~~~windthrow~~the events and 95.3% of wind-damaged area, are associated with convective storms and tornadoes (Table 7). More than a half of all ~~windthrows~~windthrow ~~areas~~events are tornado-induced with however relatively small damaged area (less than 13% of the total wind-damaged area). Non-convective storms and snowstorms are responsible for less than 5% of the area of stand-replacing ~~windthrows~~windthrow in ~~the ER~~ER. This is somewhat in contrast to Western and Central Europe, where most of ~~windthrows~~~~windthrow~~forest damage ~~are~~ is induced by non-convective wind events, namely winter storms, caused by strong extratropical cyclones (Gardiner et al., 2010; Gregow et al., 2017). Indeed, winter windstorms affects less Eastern Europe compare to Western and Central Europe (Haylock, 2011). ~~In addition, in the ER~~ER ~~and Northern Europe, ground is usually frozen during winter and prevents trees from falling because of windstorms (Suvanto et al., 2016).~~

Among 486 storm events that caused ~~windthrows~~windthrow, 381 yielded only one windthrow area (Fig. 9), primarily tornado-induced. The rest 105 storms resulted in a smaller number of ~~windthrows~~windthrow events (319) but larger damaged area — 2276.6 km^2, namely 76.8% of all damaged area. Most of these storms induced two or three successive or parallel located ~~windthrows~~windthrow areas, and only 14 of them caused ≥ 5 ~~windthrows~~~~windthrow~~ones. We found maximum of 17 separate ~~windthrows~~windthrow areas that related to one storm. We found 71 storm events result in two or more successive ~~windthrows~~windthrow areas, while 12 storm events lead to formation of two or more parallel ~~windthrows~~windthrow areas, and 22 storm events include a family of both parallel and successive

windthrowswindthrowones (fig. 36). The maximum distance between two nearest successive and two parallel windthrowswindthrow areas amounts to 150 and 26 km, respectively.

It should be noted, that a single storm may cause both tornado- and non-tornado induced windthrowswindthrow, e.g. a supercell can lead to formation of a tornado and a rear-flank downdraft (Karstens et al., 2013) both causing forest damage. In total, we found 30 storms that resulted in formation of two types of windthrowswindthrow.

We managed to match several storm events with reports at weather stations, in particular the database contains 89 such cases. Among these 89 station reports, we found eight reports with wind gusts ≥ 30 m/s, 14 reports with wind gusts 25-29 m/s, and 30 reports with wind gusts 20-24 m/s. This information have been included in the database, and can be used in further studies to estimate the critical wind speed causing windthrowswindthrow and to analyse the role of other accompanying weather phenomena, e.g. with snow, heavy rainfall, large hail, etc.

5.2 Spatial distribution of windthrowswindthrow areas

WindthrowsWindthrow eventsareas occur in the entire forest zone of the the ERER (Fig. 910). However, the highest density is observed near the 60° N and somewhat coincides with the highest percentage of forest-covered area (see Fig. 1). It is of note, that two windthrowswindthrow areas are located north of 66° N and one of them is even north of the Arctic Circle. The dominant direction of both tornado-induced and other windthrowswindthrow is SW-NE (Fig.14b15b), which is in line with the previous studies on tornado climatology in Northern Eurasia (Shikhov and Chernokulsky, 2018; Chernokulsky et al., 2020).

Three areasregions, where windthrowswindthrow have has affected more than 0.75% of forests, can be highlighted (Fig. 10a11a). Two of them are related to the catastrophic storms which occurred on 27 June 2010 and 29 July 2010. In total, these two storms have damaged 1140 km^2 of forests, which is 38.4% of the total area of stand-replacing windthrowswindthrow in the ERER in 1986–2017. The third area is located on the western slope of the Northern Ural and coincides with the largest massive of dark-coniferous forests in the the ERER (Pakhuchiy, 1997). The largest most important windthrowswindthrow events occurred here in June 1993, July 2012 and October 2016. The latter was induced by snowstorm. The relatively high frequency of windthrowswindthrow in this region was emphasized previously (Lassig and Mocalov, 2000; Shikhov and Chernokulsky, 2018; Shikhov et al., 2019). It was hypothesized that it may be related to the combination of several factors, namely widespread old-growth forests, a high precipitation rate, and large soil wetness, which all contribute to the forests wind susceptibility (Dobbertin, 2002).

The highest density of tornado-induced windthrow is found between 59° and 62° N, 48° and 56° E (Fig. 110, b), which is in a good agreement with the previous estimates (Shikhov and Chernokulsky, 2018). However, when the percentage ratio of tornado-damaged area of to the total forested area is considered is higher in the western part of the the ERER , then the western part of the ERER becomes the most affected by tornadoes (Fig. 10b11b). It is of note, that higher values of so-called convective instability indices are also observed in this region (Taszarek et al., 2018).

The species composition and age of forest stands have substantial influence on the spatial distribution of ~~windthrows~~windthrow (Dobbertin, 2002, Suvanto et al., 2016; Gregow et al., 2017). ~~However, the available data on the forests species composition for the entire ER (Fig. 1) have too coarse spatial resolution (i.e., 250 m) to overlap them with windthrows data based on 30-m Landsat images. Correct~~Using the presented dataset, estimates ~~the~~ of relationships between ~~windthrows~~windthrow area and forest stands characteristics can be carried out in future studies at a regional scale.

5.3 Temporal variability of ~~windthrows~~windthrow and storm events

We successfully determined the year of occurrence for all ~~windthrows~~windthrow events and the month of occurrence for 263 (67.9%) tornado-induced and 224 (71.5%) non-tornado-induced ~~windthrows~~windthrow events. We established the dates of occurrence for 339 ~~windthrows~~windthrow events, including 149 tornado-induced (39.2%) and 187 (59.7%) non-tornado-induced ~~windthrows~~~~windthrow~~ones. It is of note, that the dates of most ~~impacted~~ impactful large-scale ~~windthrows~~windthrow with damaged area > 10 km^2 were determined for 44 out of 49 cases (90%). ~~Windthrows~~Windthrow events with known dates have a total area of 2599 km^2, i.e., 87.7% of the total wind-damaged area.

The storm-damaged area has a relatively high inter-annual variability (Fig. ~~11~~12). The largest area of ~~windthrows~~windthrow, i.e. >1200 km^2, is found in 2010, when two exceptional storm events ~~were~~ occurred. An extremely high number of tornado-induced ~~windthrows~~windthrow events occurred in 2009 and 2017. Storm events causing ~~windthrows~~windthrow ~~are~~ have been observed every year and ranges from 2 to 36, with the maximum in 2012 and minimum in 2001. In general, annual number of ~~windthrows~~windthrow and storm events was lower before 2001 when the EEFCC data were used to identify ~~windthrows~~windthrow, and higher after 2001, when the GFC data were utilized. Annual number of ~~windthrows~~windthrow events for these periods amount to 12.1 and 30.5, respectively; in its turn, annual number of storm events amounts to 8.3 and 20.9. This temporal inhomogeneity, related to different initial data used, should be taken into account when inter-annual variability is analyzed. More details on the dataset limitations are provided in ~~Discussion~~ ~~the~~ S~~s~~ection 6.

~~Windthrows~~Windthrow events occur in the ~~the ER~~ER from May to October (Fig. ~~12~~13). ~~No winter windthrowswindthrow were was found.~~ The seasonal maximum of the number of ~~windthrows~~windthrow events is found in June — both for tornadoes and for other storm events. This is in concordance with the previous estimates on the tornado climatology (Shikhov and Chernokulsky, 2018; Chernokulsky et al., 2020). Maximum frequency of the occurrence of storm events causing ~~windthrows~~windthrow is also observed in June. Moreover, more than 90% of storm events with known dates occur in summer. It is important to note, that we failed to establish the month of ~~occurrence~~ appearance for 127 tornado-induced ~~windthrows~~windthrow areas and 98 non-tornado induced ~~windthrows~~~~windthrow~~ones, ~~with the~~which have total area of 245 km^2.

Sometimes, two or more storm events causing ~~windthrows~~windthrow occurred in ER on the same day. In total, we found seven outbreaks with more than ten ~~windthrows~~windthrow ~~events~~areas per day. The most remarkable outbreaks occurred on 18 July 2012 when nine storms resulted in 25 ~~windthrows~~windthrow ~~events~~areas, and on 7 June 2009 when five storms resulted in 24 ~~windthrows~~~~windthrow~~windthrow areas~~ones~~. However, the largest forest damage is associated with a single

storm, namely the long-lived convective storm "Asta" (Suvanto et al., 2016). This storm has passed over the northwestern part of ~~the ER~~ER and Finland on 29 July 2010 and has damaged 639 km^2 of forests in Russia.

No winter windthrow was found. It is of note, that both Landsat-based products GFC and EEFCC reveals stand-replacing windthrow area regardless of the season of its appearance. In particular, if windthrow happened in winter it would be clearly seen on image taken in subsequent vegetation period because of rather slow forest recovery process. Therefore, the revealed lack of winter windthrow is feasible due to the climatic conditions of the study area and does not associated with data limitations. In particular, winter storms from Western Europe reach the territory of Russia already weakened (Haylock, 2011), In addition, in ER and Northern Europe, while low temperatures and soil freezing also prevents trees from falling because of windstorms during winter season (Suvanto et al., 2016). According to (Suvanto et al., 2016), winter windthrow are not typical for Finland as well.

We restored the time of occurrence with 6-h accuracy for 216 ~~windthrows~~windthrow events — 136 among them using weather station reports and 80 using other data sources. We found 122 ~~windthrows~~windthrow events (56.4%) occurred between 15.00 and 21.00 of local time ~~(LT)~~, which coincides with the afternoon maximum of the development of deep convection. However, several most impactful storms, including for instance the 'Asta' storm, occurred around midnight at ~~LT~~local time. No ~~windthrows~~windthrow found between 06.00 and 10.00 local time~~LT~~ during the morning minimum of the convection diurnal cycle. The similar diurnal cycle was found for tornado events in the Northern Eurasia (Chernokulsky et al., 2020).

5.4 Geometrical parameters of ~~windthrows~~windthrow areas, elementary damaged areas, and storm tracks

Area of EDAs varies between 0.0018 to 30.9 km^2. Most of EDAs are less than 0.01 km^2 (Fig. ~~13a~~14a), but their total area is less than 10%. In turn, 1% of the largest EDAs account for 36.8% of the total area of ~~windthrows~~windthrow. Using Kolmogorov-Smirnov (K-S) test, we found that at 0.01 significant level we can reject the null hypothesis that two samples of A_{EDA} within each pair of windthrow types are drawn from the same distribution (at 0.01 level). Because of small sample size of ~~windthrows~~windthrow areas induced by non-convective storms, later in the article we will not discuss the results of K-S test to compare distributions of characteristics of this type with those of other types.

Tornado-induced ~~windthrows~~windthrow areas contain fewer ~~plots~~EDAs, than ~~other windthrows~~~~windthrow~~windthrow areas induced by strong wind (Fig. ~~13b~~14b). Particularly, most of tornado-induced ~~windthrows~~windthrow areas include 10–25 EDAs, and only 2.5% of them consist~~s~~ of more than 100 EDAs. In contrast, about 43% of non-tornado induced ~~windthrows~~windthrow areas includes more than 100 EDAs, while 5.5% of them consist~~s~~ of more than 1000 EDAs. Based on K-S test, we found that samples of number of EDAs in tornado- and convective storm induced ~~windthrows~~windthrow areas are from different distributions.

A relatively small number of severe storm events are responsible for most of the area of ~~windthrows~~windthrow (Fig. ~~14a~~15a). Indeed, the ten most destructive storm events occurred in ~~the ER~~ER over 1986-2017 damaged 1758 km^2 of forests,

namely 59.2% of the total area of ~~windthrows~~windthrow in the database. This peculiarity is less pronounced for tornado-induced ~~windthrows~~windthrow areas, since their area usually is less than 10 km^2. Particularly, ten tornadoes with the largest area damaged 96.6 km^2 of forests — 25.5% of the total tornado-damaged area. Thus, the distribution of tornado-damaged area is less skewed to high values, than the distribution of other ~~windthrows~~windthrow areas. The K-S test shows that samples of *A* for tornado- and convective storm induced ~~windthrows~~windthrow areas are from different distributions.

Length of ~~windthrows~~windthrow ranges from 0.8 km to 283.6 km (Fig. ~~14b~~15b). More than 44% of tornado-induced ~~windthrows~~windthrow areas have path length < 5 km, while path length 5-15 km is most frequent for non-tornado-induced ones. Based on K-S test, we found that samples of number of *L* for tornado- and convective storm induced ~~windthrows~~windthrow areas are from different distributions. The maximum length of storm track, consisting of several subsequent ~~windthrows~~windthrow areas, reaches 544 km. This damage track is caused by the storm on 27 June 2010. In addition, another nine storm tracks have a length exceeding 250 km — most of them are among the most destructive in terms of forest-damaged area. Such series of ~~windthrows~~windthrow with an exceptionally long path length were likely caused by derechos. Derechos are~~, i.e.~~ long-lived mesoscale convective systems producing widespread damaging winds and causing large-scale forest damage in U.S. (Johns and Hirt, 1987; Peterson, 2000), ~~and~~ Europe ~~. A few derecho events occur each year in Europe, and some of them induced catastrophic forest damage~~ (Taszarek et al., 2019), and South America (Negrón-Juárez et al., 2010). Although, not a single derecho event~~s~~ have been reported previously in Russia. A more detailed further analysis of these storm events should be carried out to confirm their nature.

Most of tornado-induced ~~windthrows~~windthrow areas have W_{max} and W_{mean} less than 200 m (Fig. ~~14~~ 15 c,d). Instead, the distribution of W_{max} of non-tornado induced ~~windthrows~~windthrow areas shifted toward larger W_{max}. In particular, 103 ~~windthrows~~windthrow areas (32.9%) have W_{max} > 1000 m. The K-S test shows that samples of both W_{max} and W_{mean} for tornado- and convective storm induced ~~windthrows~~windthrow areas are from different distributions. Width of storm tracks is several times higher than the width of ~~windthrows~~windthrow areas. Moreover, the W_{TRmax} of ~~windthrows~~windthrow areas caused by non-tornadic storms is several times higher than the W_{TRmean}. W_{TRmax} exceeds 30 km for three widest convective storms — two derechos occurred on 27 June 2010 and 29 July 2010, and one non-convective storm occurred on 7-8 August 1987.

6 ~~Discussion:~~ Data and method limitations

Due to several data and method limitations, the presented database is spatially and temporally inhomogeneous and hence incomplete. ~~The presented database likely lacks many windthrowswindthrow that occurred in ER in 1986-2017.~~ Specifically, since most of ~~windthrows~~windthrow were delineated from the GFC and EEFCC datasets, forest loss areas which are initially missed or underestimated in these datasets, could be as well missed in our database. The verification performed with the Landsat images and the HRI allows to reduce these omissions. In particular, we found several

windthrowswindthrow in small-leaved or broadleaved forests that were significantly substantially underestimated in the GFC dataset.

The efficiency of the method depends on the percentage of forest-covered area. In general, our data has highest accuracyis more complete for low-populated northern and eastern part of the the ERER, where forests cover 70-90% of the territory and dark-coniferous forests are widespread (Bartalev et al., 2016). However, some regions in the northern part of the ER are not covered by HRI which prevents from thorough verification of some windthrow areas.

In turn, the data may be less accurate In thefor southern part of the study area, the dataset is likely less complete wheresince some windthrow areas probably could becan be overlooked missed. The most reliable estimates of wind-damaged area can be obtained for low-populated northern and eastern regions of the ERER, where forests cover 70-90% of the territory (Bartalev et al., 2016) (Fig.1). In the southern part, the probability of the windthrows omission is higher (Shikhov and , Chernokulsky, 2018). In particular,

iIt is possible to miss overlook amiss windthrow if a storm or tornado passed through areas of intensive timber harvesting or agricultural lands (Shikhov and, Chernokulsky, 2018). Salvage logging performed shortly after a storm event also complicates the identification of windthrowswindthrowwind-related forest damage (Baumann et al., 2014). However, in most cases, the time interval between storm event and salvage logging in the the ERER was quite long, i.e., more than a year, except for more populated southern regions.

Currently, the proposed method requires expert verification at almost all stages, which prevents to switch it into the automatic mode. The possibility of automated searching throughout the GFC and EEFCC datasets is limited by a wide variety of geometrical shapes of windthrowswindthrow shapes and their overlapping with other forest disturbances. The data collection process requires the use of numerous and diverse sources such as the HRI from various public web services, weather station reports, eye-witness and media reports, etc.

While the algorithms for automated forest disturbances detection based on satellite data are well-developed and applied at the regional-to-global scale (Huo et al., 2019), automated attribution of forest disturbances to their causes, namely windstorms, logging, wildfires, insect outbreaks, and others, remain a critical challenge for remote sensingsatellite based forest monitoring. The spectral characteristics of various types of disturbances, e.g., windthrowswindthrow and logged areas, are often similar (Baumann et al., 2014) that complicates the automated attribution automatization of attribution. The promising approaches in this process is the complex use of spectral, temporal, and topography related metrics (Oeser et al., 2017) as well as implementing of advanced image classification/segmentation methods (Oeser et al., 2017; Liu et al., 2018; Huo et al., 2019). In future studies, such approaches can be applied to automate delineation of windthrowswindthrow areas in the ERER using satellite data of with various spatial resolution.

We have to stress Ttemporal inhomogeneity of our database, especially for small-scale windthrowswindthrow areas, comes fromdue to the following causes:

1. The use of two different Landsat-based products to search windthrow-like disturbances — the EEFCC before 2001 and the GFC after. The GFC data have higher accuracy of forest loss detection and of initial time assigning, than the

EEFCC (see Section 4.1 for details), which allows to detect more ~~windthrows~~windthrow areas. Thus, the annual number of ~~windthrows~~windthrow events 2.5 times higher in the GFC period compare to the EEFCC period.

2. After 2002-2003, the HRI had become available, which made it possible to confirm the tornadic nature of ~~windthrows~~windthrow. The observed increase in the number of tornado-induced ~~windthrows~~windthrow events after 2003 is very likely related to the appearance of the HRI.
3. The start of the Sentinel-2 mission in 2015 providing the images with a 10 m spatial resolution (Drusch et al., 2012) had also increased the possibility for windthrow identification.
4. A strong decrease in the volume of timber harvesting occurred in ~~the ER~~ER, especially in its northeastern past, after the Soviet Union dissolution (Potapov et al., 2015). This could lead to more omission of ~~windthrows~~windthrow areas in the late 1980s compare to the subsequent period because of their ~~masking out~~overlapping with ~~logging~~logged areas.
5. The number of windthrow areas and storm events has been determined with the use of arbitrary threshold values. It can be substantially change due to modification of these thresholds (see Sections 4.1.4. and 4.3. for more details). So, the data on the number of windthrow areas may be more inhomogeneous than assessment of wind-affected area.

~~The optimization of other threshold values can be evaluated in further studies that should involves ground-based data.~~Thus, the presented database should be used for assessing interannual variability with caution. Special assumptions should be made to estimate linear trends. For instance, they can be obtained for particular regions, e.g. for those with little changes of forestry practices, and for relatively large ~~windthrows~~windthrow areas, that are well-detected from both the EEFCC and the GFC data. For instance, linear trend ~~of~~ in number of ~~windthrows~~windthrow with area ≥ 1 km^2 amounts to 0.27 year^{-1} and is statistically significant at 0.05 level[1]. This increase of wind-related ~~windthrows~~~~windthrow~~forest disturbances is in line with observed increase of such characteristics as convective precipitation (Ye et al., 2017; Chernokulsky et al., 2019), convective cloudiness (Sun et al., 2001; Chernokulsky et al., 2011), convective instability indices (Riemann-Campe et al., 2009; Chernokulsky et al., 2017) in the ~~the ER~~ER in the last decades.

Currently, the proposed method requires expert verification at almost all stages, which prevents to switch it into the automatic mode. The possibility of automated searching throughout the GFC and EEFCC datasets is limited by a wide variety of windthrow shapes and their overlapping with other forest disturbance. The data collection process requires the use of numerous and diverse sources such as the HRI from various public web-services, weather station reports, eye-witness and media reports, etc.

While the algorithms for automated forest disturbance detection based on satellite data are well-developed and applied at the regional-to-global scale (Huo et al., 2019), automated attribution of forest disturbance to their causes, namely windstorms, logging, wildfires, insect outbreaks, and others, remain a critical challenge for satellite-based forest monitoring. The spectral characteristics of various types of disturbance, e.g., windthrow and logged areas, are often similar (Baumann et al., 2014)

[1] Trends were computed with the Theil–Sen estimator. Significance was obtained with the nonparametric Mann–Kendall test.

that complicates the automated attribution. The promising approaches in this process is the complex use of spectral, temporal, and topography-related metrics (Oeser et al., 2017) as well as implementing of advanced image classification/segmentation methods (Oeser et al., 2017; Liu et al., 2018; Huo et al., 2019). In future studies, such approaches can be applied to automate delineation of windthrow areas in the ER using satellite data with various spatial resolution.

7 Conclusions

The compiled GIS database contains the most complete information on a relatively large stand-replacing ~~windthrows~~windthrow areas in the forest zone of the ER in 1986 – 2017. The database contains 102747 elementary damaged areas, combined into 700 ~~windthrows~~windthrow areas, which were caused by 486 storm events. For each windthrow, we determined its type with degree of certainty, dates or date ranges, and geometrical characteristics. Database also contains weather station reports and links to additional information on storm events from the media. We included into the database only the stand-replacing ~~windthrows~~windthrow with an area > 0.05 km^2 and > 0.25 km^2 for the tornado- and non-tornado-induced ~~windthrows~~windthrow, respectively.

The total ~~area of windthrows~~windthrow area amounts to 2966 km^2, namely 0.19% of the forested area within the study region. Most of ~~windthrows~~windthrow in the ~~the ER~~ER, i.e., 82.5% of the total wind-damaged area, are related to convective squalls and downbursts, which occur mainly in June and July. The ten most impactful storms are responsible for 59.2% of the total forest damage. More than 55% of ~~windthrows~~windthrow events in the database are tornado-induced, but their contribution to total damaged area is much lower — it is less than 13%. Non-convective windstorms and snowstorms caused only 4.6% of storm-damaged area.

The largest area of ~~windthrows~~windthrow is assigned to the 2010 year, when two exceptionally destructive storm events occurred — on 27 June 2010 and 29 July 2010. An extremely high number of tornado-induced ~~windthrows~~windthrow was observed in 2009 and 2017 — 45 and 40 tornadoes, respectively.

The presented method has several limitations ~~which~~ that result~~s~~ in spatial and temporal inhomogeneity of the compiled database specifically for small-scale ~~windthrows~~windthrow areas and hence determine the dataset incompletentss. Because of influence of forest area percentage and forestry practice, such ~~windthrows~~windthrow areas can be rather missed in the southern part of the ~~the ER~~ER compare to the northern part. Because of coarser resolution of the EEFCC data and lack of the HRI, ~~such windthrows~~windthrow areas can be rather missed before 2001. The obtained increases in number of ~~windthrows~~windthrow events and ~~their~~ affected area are mainly artificial. ~~However, the positive trend is likely real for large-scale windthrows, namely for ones with the area ≥ 1 km^2.~~

Despite the incompleteness, t~~T~~he compiled database provides a valuable source of spatial and temporal information on ~~windthrows~~windthrow events in the ~~the ER~~ER~~, which previously has been incomplete~~. On the one hand, the database allows estimate the role of wind-related disturbance~~s~~ in comparison with other natural disturbance~~s~~ in forests and improve our understanding of different forest species susceptibility to windstorms. On the other hand, the database presents a unique

source of information on storm and tornado events causing ~~windthrows~~windthrow forest damage in the ~~the low-populated forest zone of the ER~~ER. It includes numerous of previously unknown storms and tornadoes, which caused forest damage, and also clarifies information on known storm events. Thus, the database ~~significantly~~ substantially contributes to the climatology of severe storms and tornadoes in the ~~the ER~~ER. Based on the compiled database, further studies may be carried out to determine the contribution of climate variability to the inter-annual variability of wind-related forest damage, and to quantify the risk of windthrow~~s events~~ in forests of the entire ER.

8 Data availability

Data are freely available at https://doi.org/10.6084/m9.figshare.12073278.~~v3~~v6. (Shikhov et al., 2020) and will be periodically updated with new and historical events.

Author contributions. ASh and ACh designed the study. ASh and ASe performed windthrow identification using satellite data. ASh and IA carried out an analysis of additional information to determine storm event types and dates. Ash and ACh, with contributions by IA, wrote the initial draft of the paper and produced the maps and figures.

Competing interests. The authors declare that they have no conflict of interest.

Acknowledgements. The study was funded by the Russian Foundation for Basic Research (projects no. 19-05-00046 and 20-35-70044). The determination of storm track characteristics was supported by the Russian Science Foundation (project no. 18-77-10076).

References

Attiwill, P. M.: The disturbance of forest ecosystems: the ecological basis for conservative management, Forest Ecology and Management, 63(2-3), 247–300, doi:10.1016/0378-1127(94)90114-7, 1994.

Ball, G. H., and Hall, D. J.: ISODATA, a Novel Method of Data Analysis and Pattern Classification, Stanford Research Institute, Menlo Park, 1965.

Bartalev, S. A., Egorov, V. A., Zharko, V. O., Lupyan, E. A., Plotnikov, D. E., Khvostikov, S. A. and Shabanov, N. V.: Satellite-based mapping of the vegetation cover of Russia, Moscow, Institute of Space Research of RAS, 208 p. 2016. (in Russian)

Baumann, M., Ozdogan, M., Wolter, P. T., Krylov, A. M., Vladimirova, N. A. and Radeloff, V. C.: Landsat remote sensing of forest windfall disturbance, Remote Sensing of Environment, 143, 171–179, doi:10.1016/j.rse.2013.12.020, 2014.

Beck, V. and Dotzek, N.: Reconstruction of near-surface tornado wind fields from forest damage, Journal of Applied Meteorology and Climatology, 49, 1517–1537, doi:10.1175/2010JAMC2254.1, 2010.

Bulygina, O. N., Veselov, V. M., Razuvaev, V. N. and Aleksandrova, T. M.: Description of the dataset of observational data on major meteorological parameters from Russian weather stations (http://meteo.ru/data/163-basicparameters), 2014.

Chernokulsky, A., Kurgansky, M., Mokhov, I., Shikhov, A., Azhigov, I., Selezneva, E., Zakharchenko, D., Antonescu, B. and Kühne, T.: Tornadoes in Northern Eurasia: from the Middle Age to the Information Era, Monthly Weather Review, 148, 3081–3111, doi: 10.1175/MWR-D-19-0251.1, 2020.

Chernokulsky, A., Kozlov, F., Zolina, O., Bulygina, O., Mokhov, I. I. and Semenov, V. A.: Observed changes in convective and stratiform precipitation in Northern Eurasia over the last five decades, Environmental Research Letters, 14, 045001–17, doi:10.1088/1748-9326/aafb82, 2019.

Chernokulsky, A V., Kurgansky, M. V. and Mokhov I. I.: Analysis of changes in tornadogenesis conditions over Northern Eurasia based on a simple index of atmospheric convective instability, Doklady Earth Sciences, 477, 1504–1509, doi:10.1134/S1028334X17120236, 2017.

Chernokulsky, A. V., Bulygina, O. N. and Mokhov, I. I.: Recent variations of cloudiness over Russia from surface daytime observations, Environmental Research Letters, 6, 035202, doi:10.1088/1748-9326/6/3/035202, 2011.

Chernokulsky, A. V., and Shikhov, A. N.: 1984 Ivanovo tornado outbreak: Determination of actual tornado tracks with satellite data, Atmospheric Research, 207, 111–121, doi:10.1016/j.atmosres.2018.02.011, 2018.

Diffenbaugh, N. S., Scherer, M., Trapp, R. J.: Robust increases in severe thunderstorm environments in response to greenhouse forcing. PNAS, 110(41), 16361–16366, doi:10.1073/pnas.1307758110, 2013.

Dmitrieva, T. G. and Peskov B. E.: Numerical forecast with the mesosynoptic specification of extremely severe squalls in the European part of Russia (Case study for June 13 and July 29, 2010), Russian Meteorology and Hydrology, 38(2), 71–79, doi:3103/S1068373913020027, 2013.

Dobbertin, M.: Influence of stand structure and site factors on wind damage comparing the storms Vivian and Lothar, Forest Snow and Landscape Research, 77(1-2), 187–205, 2002.

Doswell, C.A. and Burgess, D.W.: On some issues of United States tornado climatology. Monthly Weather Review, 116, 495–501, 1988.

Drusch, M., Del Bello, U., Carlier, S., Colin, O., Fernandez, V., Gascon, F., Hoersch, B., Isola, C., Laberinti, P., Martimort, P., Meygret, A., Spoto, F., Sy, O., Marchese, F. and Bargellini, P.: Sentinel-2: ESA's Optical High-Resolution Mission for GMES Operational Services, Remote Sensing of Environment, 120, 25–36, doi:10.1016/j.rse.2011.11.026, 2012.

Dyaduchenko, V., Pavlyukov, Y. B. and Vylegzhanin, I.: Doppler weather radars in Russia. Science in Russia, 1, 23–27, 2014. (in Russian)

Foga, S., Scaramuzza, P.L., Guo, S., Zhu, Z., Dilley, R.D., Beckmann, T., Schmidt, G.L., Dwyer, J.L., Hughes, M.J., and Laue, B. Cloud detection algorithm comparison and validation for operational Landsat data products. Remote Sensing of Environment, 194, 379-390. http://doi.org/10.1016/j.rse.2017.03.026, 2017.

Forzieri, G., Pecchi, M., Girardello, M., Mauri, A., Klaus, M., Nikolov, C., Rüetschi, M., Gardiner, B., Tomastik, J., Small, D., Nistor, C., Jonikavicius, D., Spinoni, J., Feyen, L., Giannetti, F., Comino, R., Wolynski, A., Pirotti, F., Maistrelli, F., Savulescu, I., Wurpillot-Lucas, S., Karlsson, S., Zieba-Kulawik, K., Strejczek-Jazwinska, P., Mokroš, M., Franz, S., Krejci, L., Haidu, I., Nilsson, M., Wezyk, P., Catani, F., Chen, Y.-Y., Luyssaert, S., Chirici, G., Cescatti, A. and Beck, P.S.A.: A spatially explicit database of wind disturbances in European forests over the period 2000-2018, Earth System Science Data, 12(1), 257–276, doi: 10.5194/essd-12-257-2020, 2020.

Fraser, R. H.: An analysis of large-scale forest cover disturbance in Canada (1998-2004) based on multi-temporal coarse resolution data, Proc. of the Third Int. Workshop on the Analysis of Multi-Temporal Remote Sensing Images 2005, Art. No. 1469880, 236–240, doi:10.1109/AMTRSI.2005.1469880, 2005.

Gardiner, B., Blennow, K., Carnus, J.-M., Fleischer, P., Ingemarson, F., Landmann, G., Lindner, M., Marzano, M., Nicoll, B., Orazio, C., Peyron, J.-L., Reviron, M.-P., Schelhaas, M.-J., Schuck, A., Spielmann, M. and Usbeck, T.: Destructive Storms in European Forests: Past and forthcoming Impacts, European Forest Institute, 2010.

Giglio, L., Schroeder, W., and Justice, C.O.: The collection 6 MODIS active fire detection algorithm and fire products. Remote Sensing of Environment, 178, 31–41, doi:10.1016/j.rse.2016.02.054, 2016.

Gregow, H., Laaksonen, A. and Alper, M. E.: Increasing large scale windstorm damage in Western, Central and Northern European forests, 1951–2010, Scientific Reports, 7, 46397, doi:10.1038/srep46397, 2017.

Hansen, M. C., Potapov, P. V., Moore, R., Hancher, M., Turubanova, S. A., Tyukavina, A., Thau, D., Stehman, S. V., Goetz, S. J., Loveland, T. R., Kommareddy, A., Egorov, A., Chini, L., Justice, C. O. and Townshend, J. R. G.: High-Resolution Global Maps of 21st-Century Forest Cover Change, Science, 342(6160), 850–853, doi:10.1126/science.1244693, 2013.

Hardisky, M. A., Klemas, V. and Smart, R. M.: The influence of soil salinity, growth form, and leaf moisture on the spectral radiance of Spartina alterniflora canopies. Photogramm. Eng. Remote Sens., 49, 77–83. 1983.

Haylock, M, R.: European extra-tropical storm damage risk from a multi-model ensemble of dynamically-downscaled global climate models. Natural Hazards and Earth System Sciences, 11, 2847–2857, doi:10.5194/nhess-11-2847-2011, 2011.

Huo, L.-Z., Boschetti, L. and Sparks, A.M.: Object-based classification of forest disturbance types in the conterminous United States, Remote Sensing, 11(5), 477, DOI:10.3390/rs11050477, 2019.

Johns, R. H. and Hirt, W. D.: Derechos: Widespread convectively induced windstorms. Weather and Forecasting, 2, 32–49, 1987.

Kalyakin, V. N., Smirnova, O. V., Bobrovskii, M. V., Turubanova, S. A., Potapov, P. V. and Yaroshenko, A. Y.: "History of the Eastern European forest cover", in Forests of Eastern Europe, O. V. Smirnova, Ed., 151–153, Moscow, Russia, 2004. (in Russian)

Karstens, C. D., Gallus, Jr. W.A., Lee, B. D. and Finley, C.A.: Analysis of tornado-Induced tree fall using aerial photography from the Joplin, Missouri, and Tuscaloosa-Birmingham, Alabama, Tornadoes of 2011, Journal of Applied Meteorology and Climatology, 52(5), 1049–1068, doi:10.1175/JAMC-D-12-0206.1, 2013.

Kautz, M., Meddens, A. J. H., Hall, R. J. and Arneth, A.: Biotic disturbances in Northern Hemisphere forests – a synthesis of recent data, uncertainties and implications for forest monitoring and modelling, Global Ecology and Biogeography, 26(5), 533–552, doi: 10.1111/geb.12558, 2017.

Koroleva, N. V., and Ershov, D. V.: Estimation of error in determining the forest windfall disturbances area on high spatial resolution space images of LANDSAT-TM. In: Current Problems in Remote Sensing of the Earth From Space, 9, 80–86, 2012. (in Russian)

Korznikov, K. A., Kislov, D. E., Belyaeva, N. G.: The first record of catastrophic windthrow in boreal forests of South Sakhalin and the South Kurils (Russia) during October 2015 tropical cyclones, Botanica Pacifica, 8(1), 31–38, doi:10.17581/bp.2019.08115, 2019.

Köster, K., Voolma, K., Jõgiste, K., Metslaid, M. and Laarmann, D.: Assessment of tree mortality after windthrow using photo-derived data, Annales Botanici Fennici, 46(4), 291–298, doi:10.5735/085.046.0405, 2009.

Krylov, A. M., Malahova, E. G. and Vladimirova, N. A.: Identification and assessment of forest areas damaged by windfalls in 2009–2010 by means of remote sensing, Bull. Of Saint-Petersburg Academy of Forest Management, 200, 197–207, 2012. (in Russian)

Landsat Collection 1. Available from: https://www.usgs.gov/land-resources/nli/landsat/landsat-collection-1?qt-science_support_page_related_con=1#qt-science_support_page_related_con (Accessed 2 April 2020), 2019.

Lassig, R. and Moĉalov, S. A.: Frequency and characteristics of severe storms in the Urals and their influence on the development, structure and management of the boreal forests, Forest Ecology and Management, 135, 179–194, doi:10.1016/S0378 -1127(00)00309-1, 2000

Liu, Z., Peng, C., Work, T., Candau, J.-N., Desrochers, A., Kneeshaw, D.: Application of machine-learning methods in forest ecology: Recent progress and future challenges, Environmental Reviews, 26(4), 339–350. DOI:10.1139/er-2018-0034, 2018.

Los Angeles Times, 1998. 6 Die, 122 Hurt as Windy Storm Rips Up Moscow, Available from: https://www.latimes.com/archives/la-xpm-1998-jun-22-mn-62451-story.html (Accessed 3 April 2020).

Local Polynomial Interpolation – Help. ArcGIS Desktop, Available from: http://desktop.arcgis.com/en/arcmap/latest/tools/geostatistical-analyst-toolbox/local-polynomial-interpolation.htm (Accessed 3 April 2020).

Millar, C. I. and Stephenson, N. L.: Temperate forest health in an era of emerging megadisturbance, Science, 349(6250), 823–826, doi:10.1126/science.aaa9933, 2015.

Negrón-Juárez, R.I., Chambers, J.Q., Guimaraes, G., Zeng, H., Raupp, C.F.M., Marra, D.M., Ribeiro, G.H.P.M., Saatchi, S.S., Nelson, B.W., Higuchi, N., Widespread Amazon forest tree mortality from a single cross-basin squall line event. Geophysical Research Letters 37, 1–5. https://doi.org/10.1029/2010GL043733, 2010.

Nilsson, C., Stjernquist, I., Bärring, L., Schlyter, P., Jönsson, A.M., and Samuelsson, H.: Recorded storm damage in Swedish forests 1901-2000, Forest Ecology and Management, 199(1), 165–173. doi:10.1016/j.foreco.2004.07.031, 2004.

Oeser, J., Pflugmacher, D., Senf, C., Heurich, M. and Hostert, P.: Using intra-annual Landsat time series for attributing forest disturbance agents in Central Europe, Forests, 8(7), Art. No. 251, doi:10.3390/f8070251, 2017.

Overpeck, J. T., Rind, D., and Goldberg, R.: Climate-induced changes in forest disturbance and vegetation, Nature, 343(6253), 51–53, doi:10.1038/343051a0, 1990.

Pakhuchiy, V.V.: Virgin stands of coniferous taiga in the far southeastern Komi republic, Polar Geography, 21(3), 213–223. doi: 10.1080/10889379709377626, 1997.

Peterson, C. J.: Catastrophic wind damage to North American forests and the potential impact of climate change, Science of the Total Environment, 262, 287–311. doi:10.1016/S0048-9697(00)00529-5

Petukhov, I. N., and Nemchinova, A. V.: Windthrows in forests of Kostroma oblast and the neighboring lands in 1984-2011, Russian Journal of Forest Science, 6, 16–24, 2014. (in Russian)

Potapov, P. V., Turubanova, S. A., Tyukavina, A., Krylov, A. M., McCarty, J. L., Radeloff, V. C. and Hansen, M. C.: Eastern Europe's forest cover dynamics from 1985 to 2012 quantified from the full Landsat archive, Remote Sensing of Environment, 159, 28–43, doi:10.1016/j.rse.2014.11.027, 2015.

Radler, T., Groenemeijer, P., Faust, E., Sausen, R. and Púčik, T.: Frequency of severe thunderstorms across Europe expected to increase in the 21st century due to rising instability, NPJ Climate and Atmospheric Science, 30, doi:10.1038/s41612-019-0083-7, 2019.

Riemann-Campe. K., Fraedrich. K. and Lunkeit. F.: Global climatology of convective available potential energy (CAPE) and convective inhibition (CIN) in ERA-40 reanalysis, Atmospheric Research, 93, 534–545, doi:10.1016/j.atmosres.2008.09.037, 2009.

Sayn-Wittgenstein, L., and Wightman, J. M.: Landsat application in Canadian forestry. In: Proceeding of the 10th Int. Symp. on Remote Sensing of Environment, 2, 1209–1218, 1975.

Schaefer, J.T.~~,~~ and Edwards, R.~~,~~ The SPC tornado/severe thunderstorm database. In: Preprints, 11th Conf. on Applied Climatology. Amer. Meteor. Soc, Dallas, TX Available online at. https://ams.confex.com/ams/99annual/abstracts/1360.htm (6.11), 1999.

Schelhaas M. J., Nabuurs G. J., and Schuck A.: Natural disturbances in the European forests in the 19th and 20th centuries, Global Change Biology, 9(11), 1620–1633, doi:10.1046/j.1365-2486.2003.00684 .x, 2003.

Schmoeckel, J., and Kottmeier, C.: Storm damage in the Black Forest caused by the winter storm "Lothar" – Part 1: Airborne damage assessment, Natural Hazards Earth System Sciences, 8, 795–803, doi:10.5194/nhess-8-795-2008, 2008.

Seidl, R., Schelhaas, M.-J. and Lexer, M. J.: Unraveling the drivers of intensifying forest disturbance regimes in Europe, Global Change Biology, 17(9), 2842–2852, doi:10.1111/j.1365-2486.2011.02452.x, 2011.

Seidl, R., Schelhaas, M.-J., Rammer, W. and Verkerk, P. J.: Increasing forest disturbances in Europe and their impact on carbon storage, Nature Climate Change, 4(9), 806–810, doi:10.1038/nclimate2318, 2014.

Seidl, R., Thom, D., Kautz, M., Martin-Benito, D., Peltoniemi, M., Vacchiano, G., Wild, J., Ascoli, D., Petr, M., Honkaniemi, J., Lexer, M.J., Trotsiuk, V., Mairota, P., Svoboda, M., Fabrika, M., Nagel T.A. and Reyer, C. P. O.: Forest disturbances under climate change, Nature Climate Change, 7(6), 395–402. doi:10.1038/nclim ate33 03, 2017.

Senf, C., Pflugmacher, D., Zhiqiang, Y., Sebald, J., Knorn, J., Neumann, M., Hostert, P. and Seidl, R.: Canopy mortality has doubled in Europe's temperate forests over the last three decades, Nature Communications, 9(1), 4978, doi:10.1038/s41467-018-07539-6, 2018.

Shamin, S. I., Buhonova, L. K., and Sanina, A. T.: Database of hazardous and unfavourable hydrometeorological events that did damage to the economy and population of the Russian Federation. http://meteo.ru/english/climate/weather_and_hazards.php. 2019.

Skvortsova, E. B., Ulanova, N. G., and Basevich, V. F.: The ecological role of windthrow, Moscow, 1983. (in Russian)

Shikhov, A. N., and Chernokulsky, A. V.: A satellite-derived climatology of unreported tornadoes in forested regions of northeast Europe, Remote Sensing of Environment, 204, 553–567, doi:10.1016/j.rse.2017.10.002, 2018.

Shikhov, A., Chernokulsky, A., Azhigov, I., and Semakina, A.: A satellite-derived database for stand-replacing windthrow events in boreal forests of European Russia in 1986–2017~~A satellite-derived database for stand-replacing windthrows in boreal forests of the European Russia in 1986-2017~~. figshare. Dataset. ~~https://doi.org/10.6084/m9.figshare.12073278.v3~~https://doi.org/10.6084/m9.figshare.12073278.v6, 2020.

Shikhov, A. N., Chernokulsky, A. V., Sprygin, A. A., and Azhigov I. O.: Identification of mesoscale convective cloud systems with tornadoes using satellite data, Sovremennye problemy distantsionnogo zondirovaniya Zemli iz kosmosa, 16(1), 223–236, doi:10.21046/2070-7401-2019-16-1-223-236, 2019.

Shikhov, A. N., Perminova E. S., and Perminov S. I.: Satellite‐based analysis of the spatial patterns of fire and storm-related forest disturbances in the Ural region, Russia, Natural Hazards, 97, 283–308, doi:10.1007/s11069-019-03642-z), 2019.

Shikhov A. N., and Zaripov A. S.: Long-term dynamics of fire- and wind-related forest losses in northeast European Russia from satellite data, Sovremennye problemy distantsionnogo zondirovaniya Zemli iz kosmosa, 15(7), 114–128, doi:10.21046/2070-7401-2018-15-7-114-128, 2018. (in Russian)

Sun, B., Groisman, P. Y. and Mokhov I. I.: Recent Changes in Cloud-Type Frequency and Inferred Increases in Convection over the United States and the Former USSR, Journal of Climate, 14, 1864–1880, doi:10.1175/1520-0442(2001)014<1864:RCICTF>2.0.CO;2, 2001.

Suvanto, S., Henttonen, H. M., Nöjd, P., and Mäkinen, H.: Forest susceptibility to storm damage is affected by similar factors regardless of storm type: Comparison of thunder storms and autumn extra-tropical cyclones in Finland, Forest Ecology and Management, 381, 17–28, doi: 10.1016/j.foreco.2016.09.005, 2016.

Taszarek, M., Brooks, H. E., Czernecki, B., Szuster, P. and Fortuniak, K.: Climatological Aspects of Convective Parameters over Europe: A Comparison of ERA-Interim and Sounding Data, Journal of Climate, 31, 4281–4308, doi: 10.1175/JCLI-D-17-0596.1, 2018.

Taszarek, M., Pilguj, N., Orlikowski, J., Surowiecki, A., Walczakiewicz, S., Pilorz, W., Piasecki, K., Pajurek, L. and Półrolniczak, M.: Derecho evolving from a Mesocyclone-A Study of 11 August 2017 severe weather outbreak in Poland: Event analysis and high-resolution simulation, Monthly Weather Review, 147(6), 2283–2306, doi:10.1175/MWR-D-18-0330.1, 2019.

Ulanova, N.G.: The effects of windthrow on forests at different spatial scales: a review. Forest Ecology and Management 135, 155–167. doi:10.1016/S0378-1127(00)00307-8, 2000.

Usbeck, T., Waldner, P., Dobbertin, M., Ginzler, C., Hoffmann, C., Sutter, F., Steinmeier, C., Volz, R., Schneiter, G. and Rebetez, M.: Relating remotely sensed forest damage data to wind data: Storms Lothar (1999) and Vivian (1990) in Switzerland, Theoretical and Applied Climatology, 108(3-4), 451–462, doi:10.1007/s00704-011-0526-5, 2012.

Usbeck, T., Wohlgemuth, T., Dobbertin, M., Pfister, C., Bürgi, A., Rebetez, M.: Increasing storm damage to forests in Switzerland from 1858 to 2007, Agricultural and Forest Meteorology, 150(1), 47–55, doi: 10.1016/j.agrformet.2009.08.010, 2010.

van Lierop, P., Lindquist, E., Sathyapala, S., Franceschini, G.: Global forest area disturbance from fire, insect pests, diseases and severe weather events, Forest Ecology and Management, 352, 78–88, doi:10.1016/j.foreco.2015.06.010, 2015.

Wang, F., and Xu, Y. J.: Comparison of remote sensing change detection techniques for assessing hurricane damage to forests. Environmental Monitoring and Assessment, 162, 311–326, doi:10.1007%2Fs10661-009-0798-8, 2010.

Wang, W., Qu, J.J., Hao, X., Liu, Y., Stanturf, J. A.: Post-hurricane Forest damage assessment using satellite remote sensing. Agricultural and. Forest. Meteorology, 150, 122–132. doi:10.1016/j.agrformet.2009.09.009, 2010.

Westerling, A. L.: Increasing western US forest wildfire activity: Sensitivity to changes in the timing of spring, Philosophical Transactions of the Royal Society B: Biological Sciences, 371(1696), Art. No. 20150178, doi:10.1098/rstb.2015.0178, 2016.

Wulder, M. A., Masek, J. G., Cohen, W. B., Loveland, T. R., and Woodcock, C. E.: Opening the archive: how free data has enabled the science and monitoring promise of Landsat, Remote Sensing of Environment, 122, 2–10, doi:10.1016/j.rse.2012.01.010, 2012.

WWF Russia's Boreal Forests. Forest Area Key Facts & Carbon Emissions from Deforestation, Available from: http://assets.panda.org/downloads/russia_forest_cc_final_13nov07.pdf (Accessed 3 April 2020).

Ye, H., Fetzer E. J., Wong. S., and Lambrigtsen B. H.~~;~~ Rapid decadal convective precipitation increase over Eurasia during the last three decades of the 20th century, Science Advances, 3, e1600944, doi: 10.1126/sciadv.1600944, 2017.

1005

Field name	Field alias	Type, length	Description
OBJECTID	OBJECTID	Object ID	Index number of EDA
ID	Windthrow ID	Short	Windthrow ID
Storm_ID	ID of storm event	Short	ID of a storm event
Area	Area (km^2)	Float	EDA area (km^2)

Table 1: Attribute table of the GIS layer of elementary damaged areas (EDAs).

1010

Field name	Field alias	Type, length	Description
OBJECTID	OBJECTID	Object ID	Index number of windthrow
ID	Windthrow ID	Short	A windthrow ID
Storm_ID	ID of storm event	Short	ID of storm event
Storm_type	Type of storm	String, 10	A type of a storm that caused the windthrow: convective windstorm, tornado, non-convective windstorm, or snowstorm
Certainty	Event certainty degree	String, 20	The degree of certainty of storm type determination: high or medium
Source_1	Data source for windthrow delineation	String, 50	Data source for windthrow delineation
Source_2	Data source for windthrow type defining	String, 100	Data source for windthrow type defining
Year	Year	Short integer	The year of the windthrow event
Month	Month	Short integer	The month of the windthrow event
Date	Storm event date	String, 20	The date of storm event
Date_1	Date of first image	Date	The date of the last Landsat/Sentinel-2 image that lack the windthrow
Date_2	Date of second image	Date	The date of the first Landsat/Sentinel-2 image, by which the windthrow was detected
Time_range	Time range	String, 50	Time range of storm event (UTC)
Time_Src	Data source for determine storm time range	String, 255	Data source or URL that was used to determine the time range of a storm event
N_polygons	Number of single-part polygons	Short	Number of single-part polygons
Area	Area (km^2)	Float	Windthrow area (km^2)
Length	Path length (km)	Float	Length of windthrow (km)
Mean_width	Mean width of windthrow excluding gaps (m)	Float	Mean width of windthrow (m) — for damaged area only
Max_width	Max width of windthrow excluding gaps (m)	Float	Maximum width of windthrow (m) —for damaged area only
Mean_w_2	Mean width of windthrow with gaps (m)	Float	Mean width of windthrow including gaps (m)
Max_w_2	Max width of windthrow with gaps (m)	Float	Maximum width of windthrow including gaps (m)
Direction	Direction of windthrow	String, 10	Elongated direction of windthrow, i.e. direction of storm movement
Near_WS	WMO ID of the weather station	Long	WMO ID of the nearest weather station — if the distance between windthrow and weather station is less than 50 km or weather station located on the storm track
WS_dist	Distance to weather station	Float	Distance to the nearest weather station (km)

	(km)		
Wind_gust	Wind gust (m/s)	Short	Maximum wind gust that measured by the weather station on a day when windthrow occurred
Gust_time	Wind gust time (UTC)	Short	Time of wind gust report (UTC) with 3-hour accuracy
Sum_prec	Precipitation amount	Short	Precipitation amount (only for events with heavy rainfall ≥ 30 mm/12h)
WS_comment	Additional data from weather station	String, 100	Additional data on the storm event reported by the weather station, i.e. heavy rainfall (≥ 30 mm/12h), large hail, tornado
URL	External URL	String, 100	URL of the additional data source (newspaper report or video)

Table 2: Attribute table of the GIS layer of ~~windthrows~~windthrow in the forest zone of ER (1986-2017).

1015

Field name	Field alias	Type, length	Description
OBJECTID	OBJECTID	Object ID	Index number of a storm track
Storm_ID	ID of storm event	Short	ID of a storm event
Count	Number of windthtows	Short	Number of ~~windthrows~~windthrow caused by a storm event
Area_tr	Area (km^2)	Float	Total damaged area (km^2)
Length_tr	Path length (km)	Float	Total path length with gaps, km)
Mean_w_tr	Mean width of storm track (m)	Float	Mean width of storm track (km)
Max_w_tr	Max width of storm track (m)	Float	Maximum width of storm track (km)

Table 3: Attribute table of the GIS layer of storm events tracks.

Degree of certainty	~~Windthrows~~Windthrow induced by		
	Tornado	Convective storm	Non-convective storm
High (>95% likelihood of occurrence)	Independent confirmation of the tornado event (photo, video, etc.); well-detected rotation of the fallen trees (counterclockwise usually); all three additional signatures are confirmed (in the lack of the HRI)	Elongated, but amorphous (mosaic) spatial structure of forest disturbances and a varying degree of forest damage; the direction of the fallen trees generally corresponds to a storm track direction	Independent confirmation of non-convective storm causing windthrow by weather station or/and eye-witness/newspaper report;
Medium (50–95% likelihood)	The HRI are unavailable or do not allow to determine the direction of the fallen trees and only two out of three additional signature are confirmed.	HRI are unavailable or do not allow to determine the direction of the fallen trees; quasi-linear structure of a windthrow without turns of a track, and a ratio of length and width < 10:1	The date of a storm event indicate a low probability of a convective storm (e.g., autumn season) and lack of elongation along the wind direction (especially for ~~windthrows~~windthrow induced by snowstorms)

Table 4: The signatures used to assess the degree of certainty of windthrow type determination.

Number	Total area (GFC/HRI), km^2	*A* (overlapped), km^2	Producer's accuracy, %	User's accuracy, %	*L*, km (GFC/HRI)	W_{mean}, m (GFC/HRI)	W_{max}, m (GFC/HRI)
1	6.08/6.49	5.04	77.6	82.8	9.4/9.4	588/612	1433/1467
2	4.36/5.11	2.98	58.5	68.5	15.9/17.2	290/405	860/1798
3	1.74/1.54	0.75	48.7	43.2	42.5/42.5	104/87	542/390
4	1.55/1.31	0.79	60.3	51.3	9.0/9.1	178/152	681/593
5	1.33/0.92	0.71	77.0	53.6	6.7/6.8	220/145	638/510
6	1.00/0.76	0.41	53.9	41.1	21.8/21.8	86/70	343/250
7	0.88/0.76	0.41	53.9	46.6	14.6/14.7	112/97	458/382
8	0.42/0.32	0.19	59.7	44.5	7.4/7.2	85/53	233/179
9	0.27/0.14	0.11	77.2	41.7	2.1/2.1	136/79	306/264
10	0.26/0.25	0.15	61.4	60.0	9.4/9.4	86/59	188/206

Table 5: Comparison of ~~windthrows~~windthrow geometrical parameters estimated using the GFC and the HRI data.

Number	A, km^2 (EEFCC/HRI),	A (overlapped), km^2	Producer's accuracy	User's accuracy	L, km (EEFCC/HRI)	W_{mean}, m (EEFCC/HRI)	W_{max}, m (EEFCC/HRI)
1	3.11/4.18	2.58	82.96	61.72	14.6/14.2	308/257	963/748
2	1.59/2.35	1.25	78.62	53.19	16.8/16.9	186/148	568/491
3	3.48/3.82	2.68	77.01	70.16	14.2/14.9	305/288	1507/1269
4	0.82/1.11	0.67	81.71	60.36	10.3/10.4	166/158	367/332
5	1.09/1.28	0.94	86.24	73.44	9.5/10.1	171/161	380/291

Table 6: Comparison of ~~windthrows~~windthrow geometrical parameters estimated using the EEFCC and the HRI data.

Windthrow type	Degree of certainty	Number of ~~windthrows~~windthrow	Damaged area, km^2
Convective storm induced	High	270	2371.6
	Medium	25	7.6
Tornado-induced	High	295	300.4
	Medium	92	79.2
Non-convective storm induced	High	12	131.8
	Medium	6	5.9
Total	High	577	2803.8
	Medium	123	92.7

Table 7: Total number of ~~windthrows~~windthrow of different types and corresponding forest damaged area.

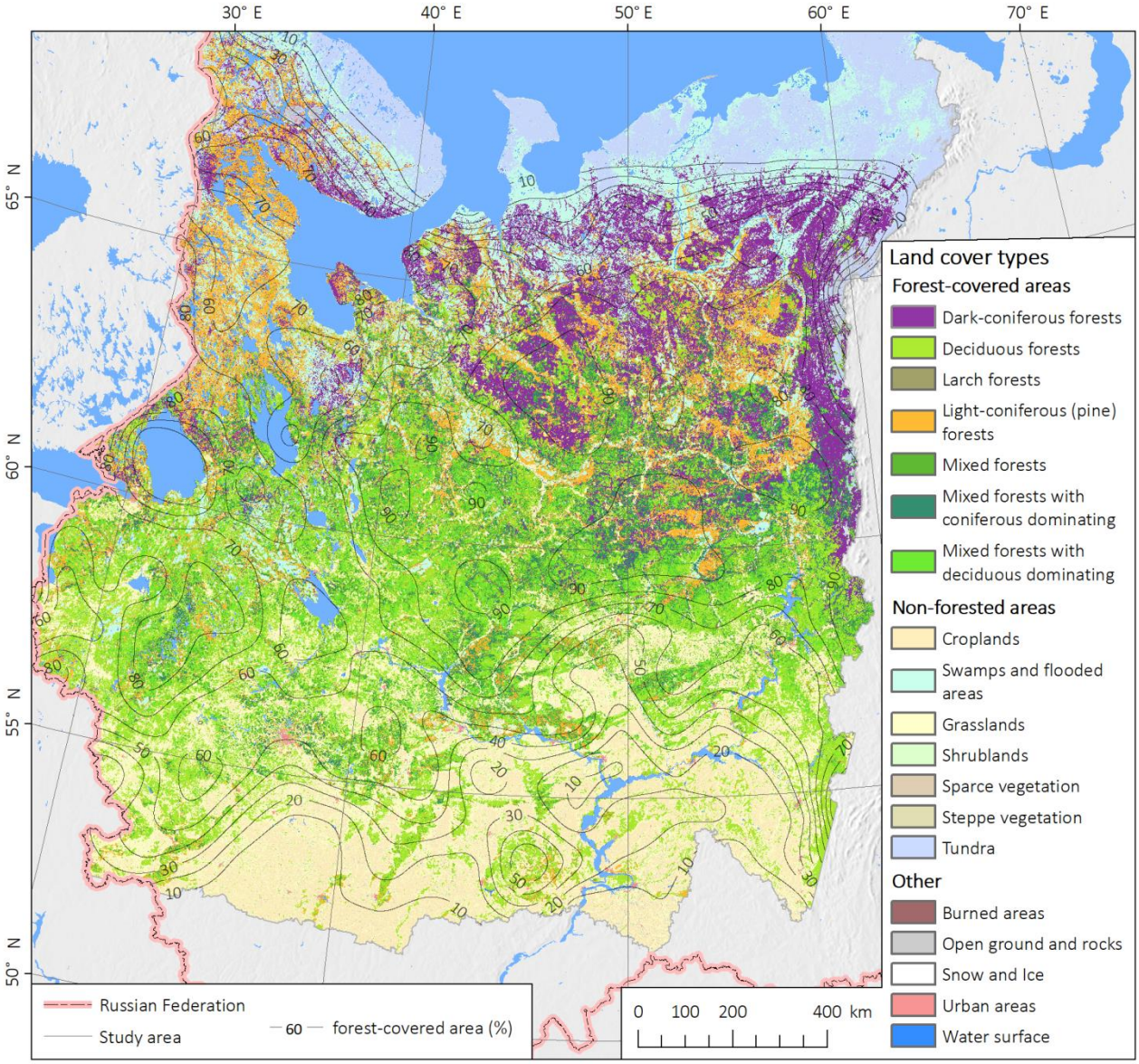

1035 **Figure 1: Land cover types within the study area,** according to the map of vegetation cover of Russia, developed by the Space Research Institute of the Russian Academy of Sciences (Bartalev et al., 2016).

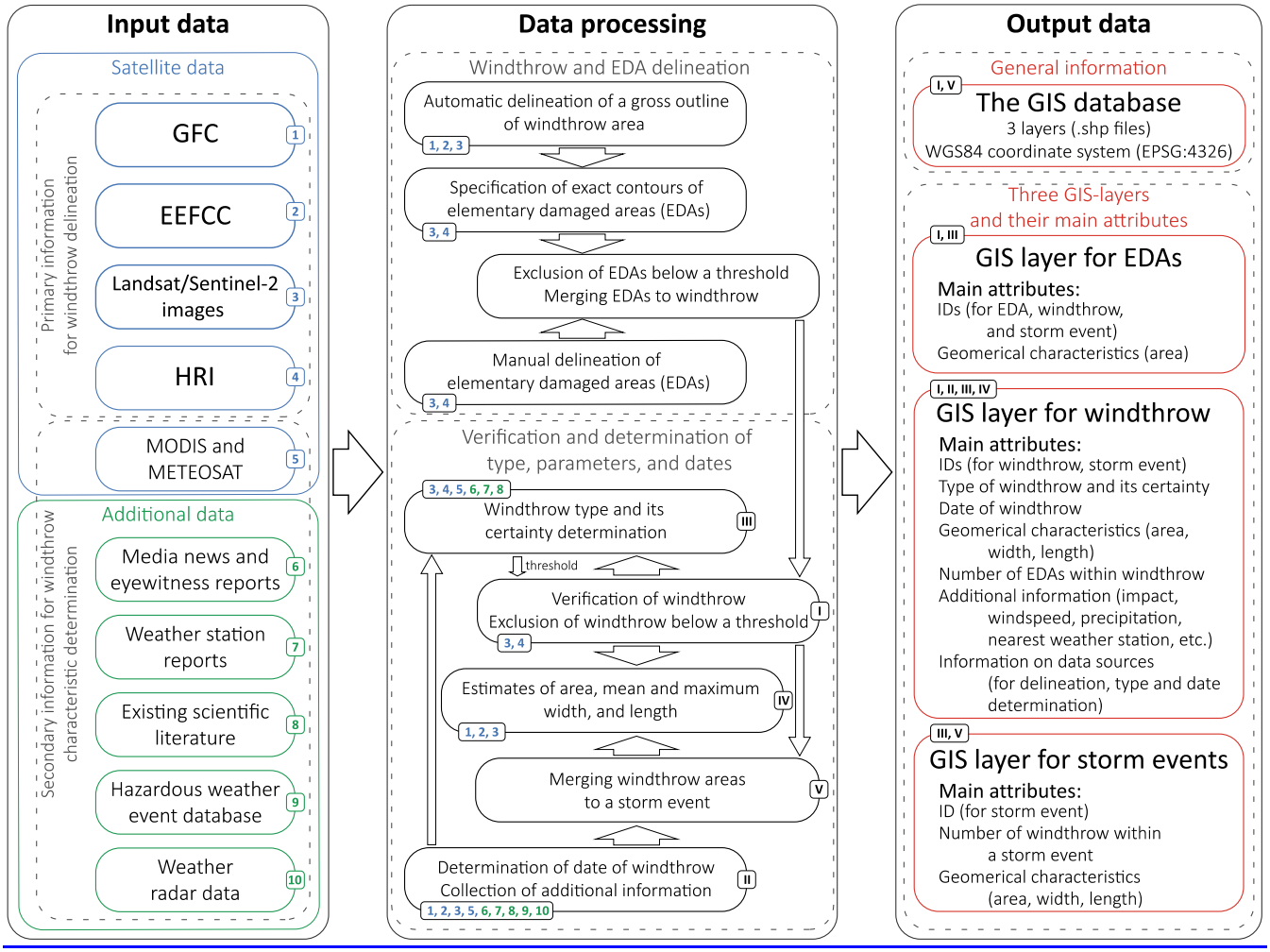

Figure 2: Workflow used for windthrow delineation and attribution.

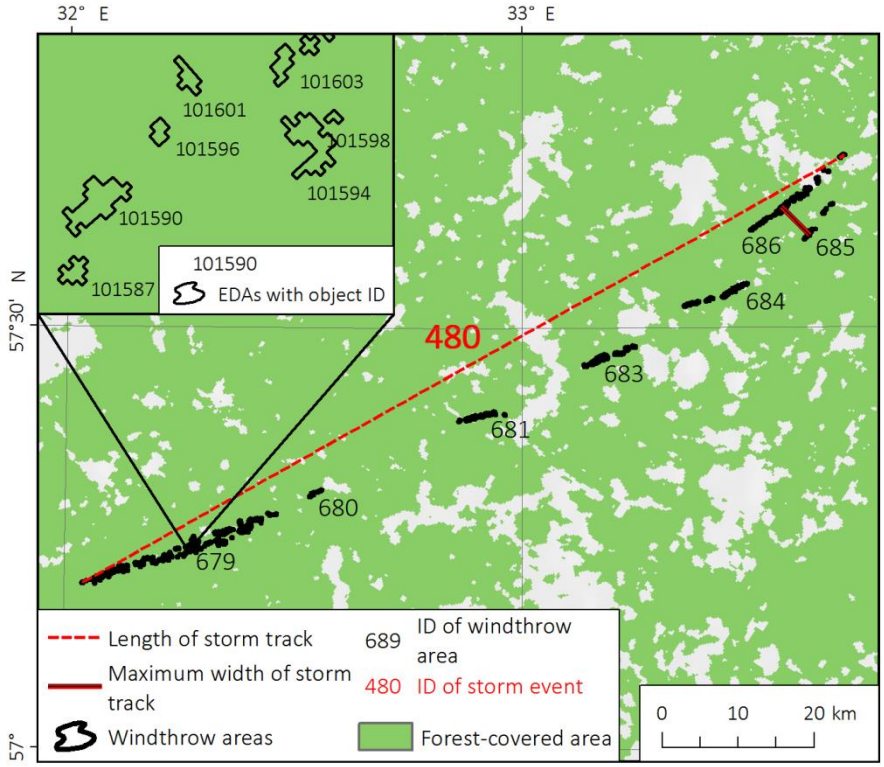

Figure 3~~6~~: An example of three hierarchical levels of the database for the event occurred on 2 Aug 2017. A scheme for the determination of geometrical parameters of a storm event is also shown. Parallel (680, 681) and successive (684, 689, 682, 678) locations of windthrow areas ~~is~~are ~~shown~~indicated as well.

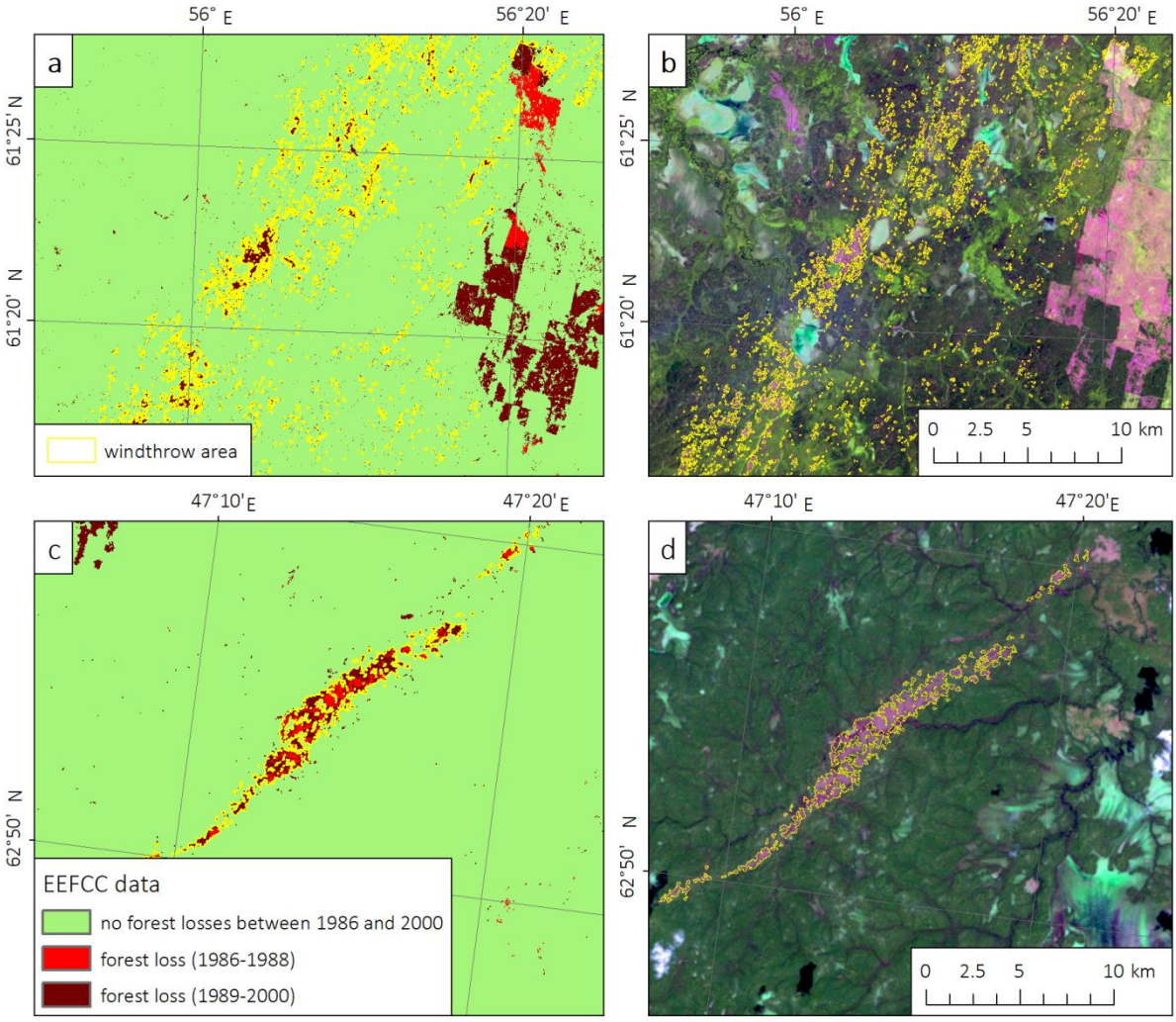

Figure 4~~3~~: Delineation of (a, b) storm- and (c, d) tornado-induced ~~windthrows~~windthrow occurred on 4 July 1992 and 24 July 1988 respectively based on (a, c) the EEFCC dataset and (b, d) its subsequent verification by the Landsat images, created as a combination of the TM3 (0.66 µm), TM4 (0.85 µm), and TM5 (1.65 µm) spectral bands.

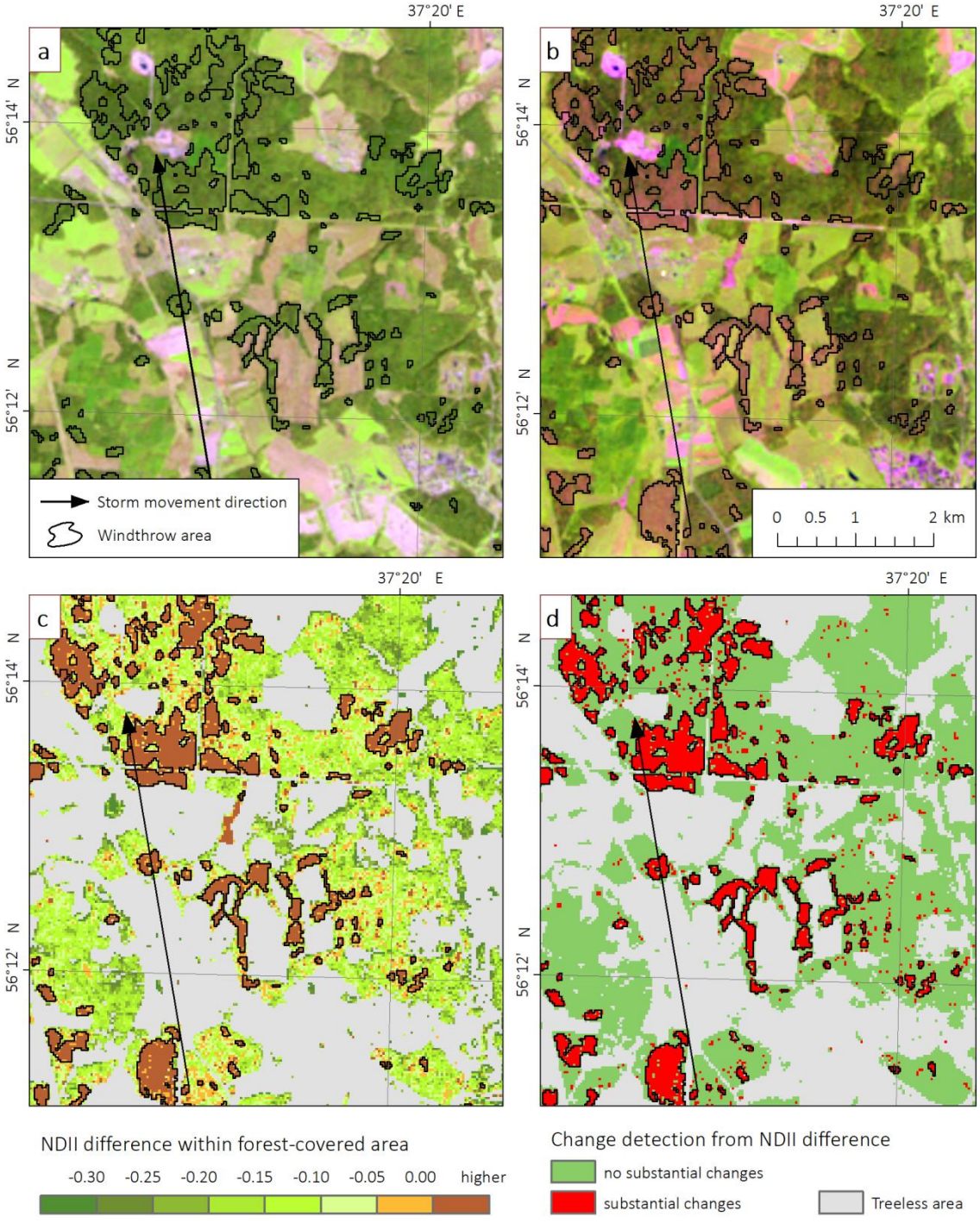

Figure 54: Windthrow delineation the windstorm occurred on 21 June 1998 in Moscow region based on the NDII difference method: the Landsat-5 images obtained (a) before and (b) after the storm event — 11 May 1998 and 30 July 1998, respectively; (c) the NDII difference within forest-covered area and (d) the areas with the substantial decrease of NDII.

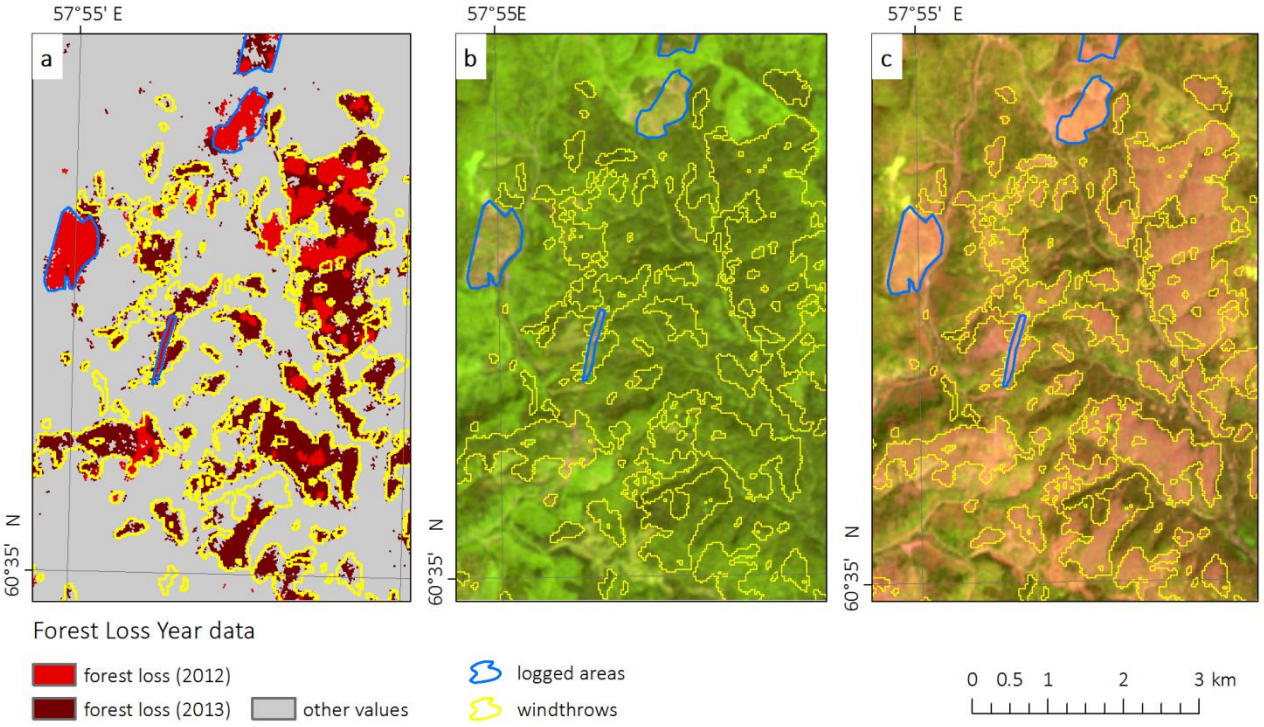

Figure 65: Separation of the windthrow occurred on 18 July 2012 from logged areas based on (a) the GFC data on forest losses, and Landsat images obtained (b) before (i.e., 8 July 2012) and (c) after (i.e., 18 Aug 2012) the storm event.

1060

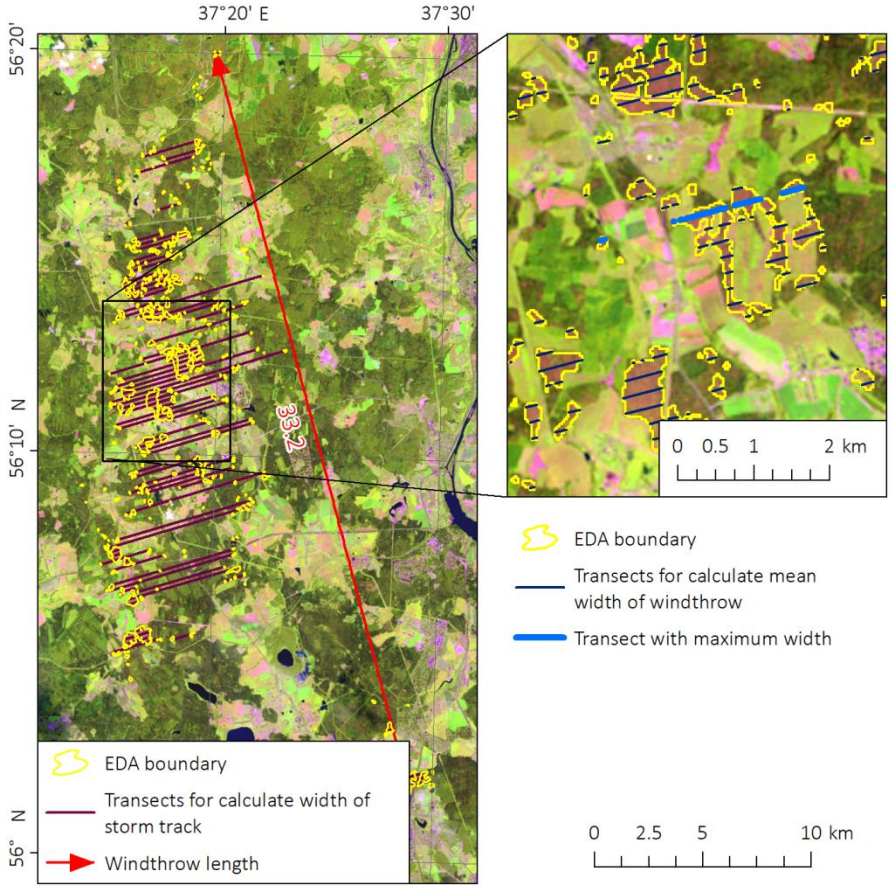

Figure ~~6~~7: A scheme for the determination of geometrical parameters of a windthrow based on the Landsat image using the example of the windthrow in the Moscow region occurred on 21 June 1998.

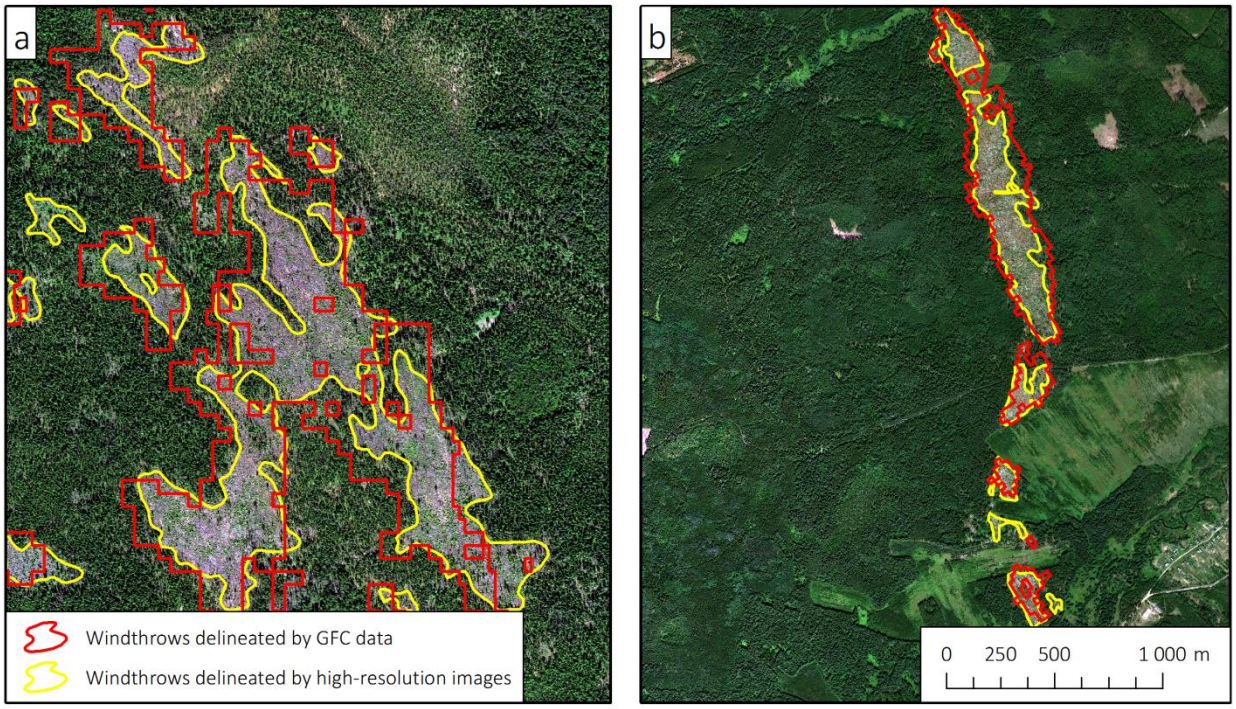

Figure ~~7~~8: Overlapping of windthrow areas that extracted from the GFC dataset and delineated manually using the HRI for (a) convective-storm induced windthrow (18 July 2012), and (b) tornado-induced windthrow (June 2011).

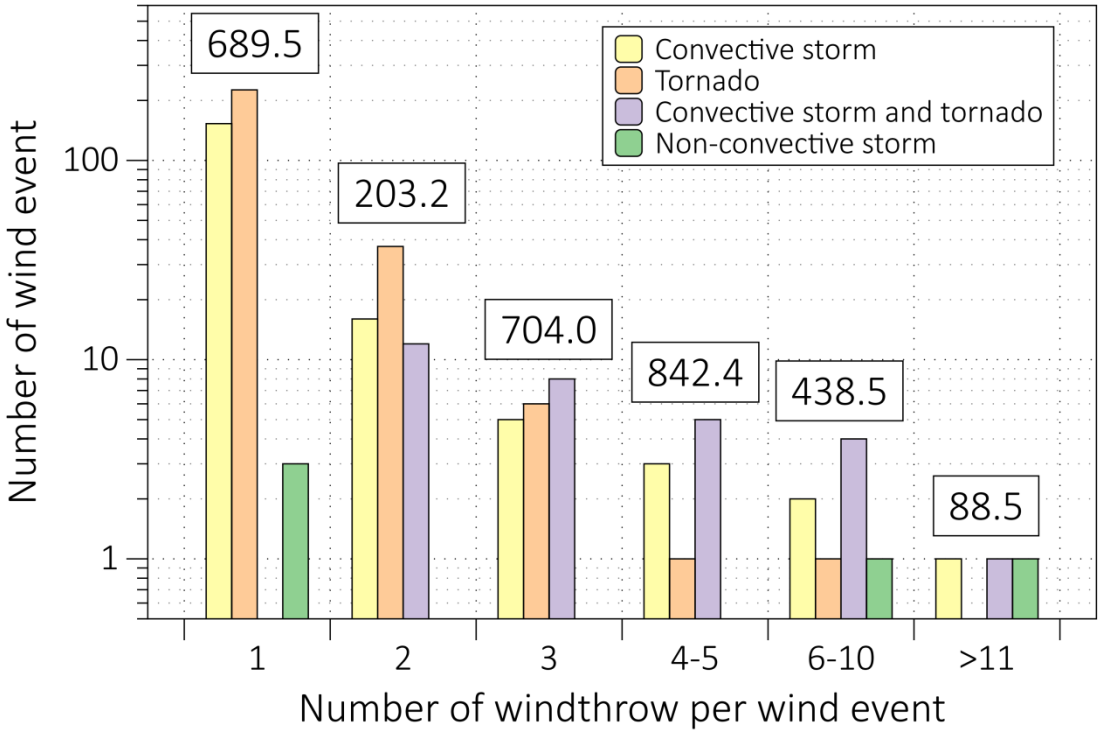

Figure ~~8~~9: Number of ~~windthrows~~windthrow per one storm event. Total damaged area (in km^2) corresponding to all type of ~~windthrows~~windthrow is shown in box for each category.

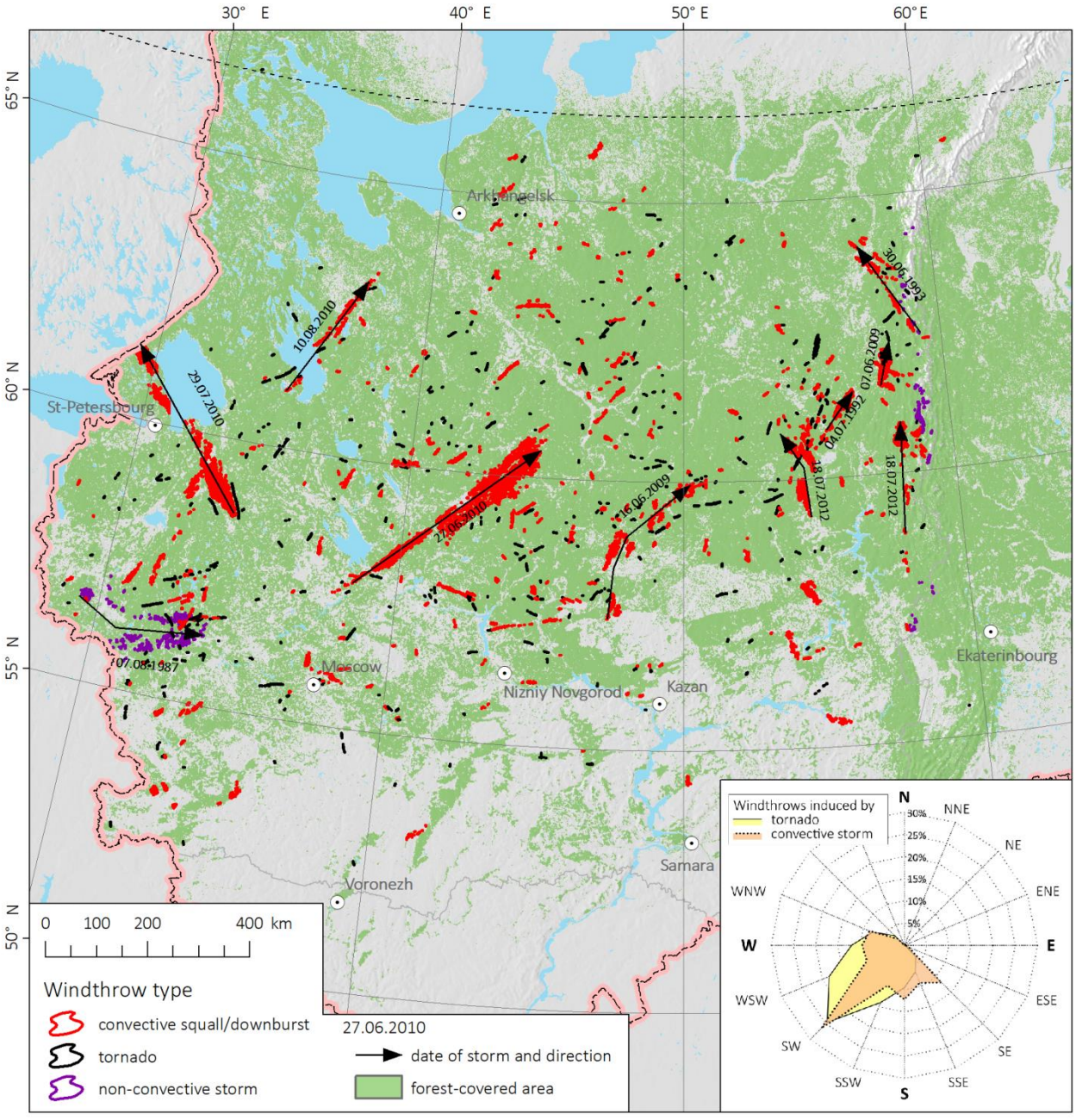

Figure ~~9~~10: Spatial distribution of stand-replacing ~~windthrows~~windthrow in ~~the ER~~ER in 1986-2017. The ten most catastrophic ~~windthrows~~windthrow with the largest damaged area are shown by arrows and indicated by the corresponding dates of ~~windthrows~~windthrow. Forest-covered area is estimated according to the data from Bartalev et al. (2016). The inset shows the direction from which ~~windthrows~~windthrow originate.

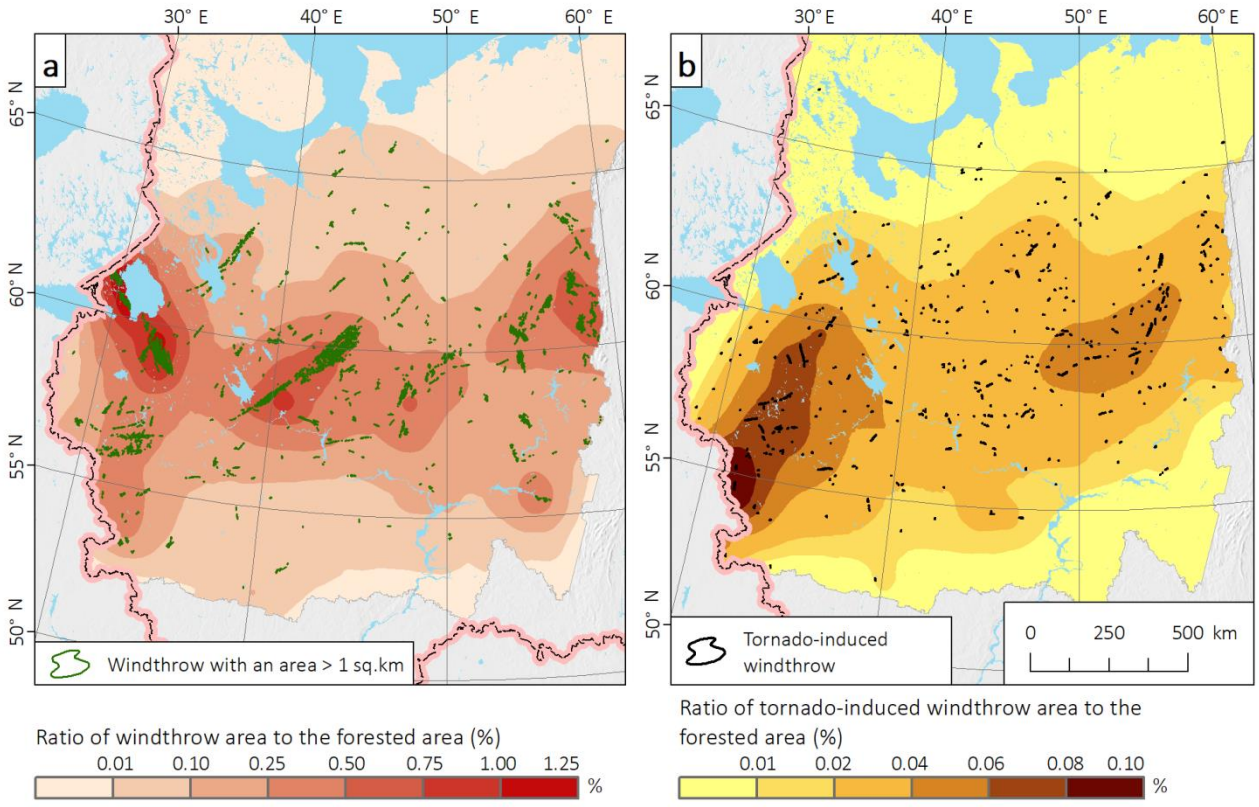

Figure 1~~0~~1: Ratio of damaged area to the forest-covered area for (a) all ~~windthrows~~windthrow and (b) tornado-induced ~~windthrows~~windthrow only. The ratio of ~~windthrows~~windthrow area to the forest-covered area was calculated for 100 km^2 cell and then interpolated with local polynomial interpolation method in the ArcGis Geostatistical Analyst.

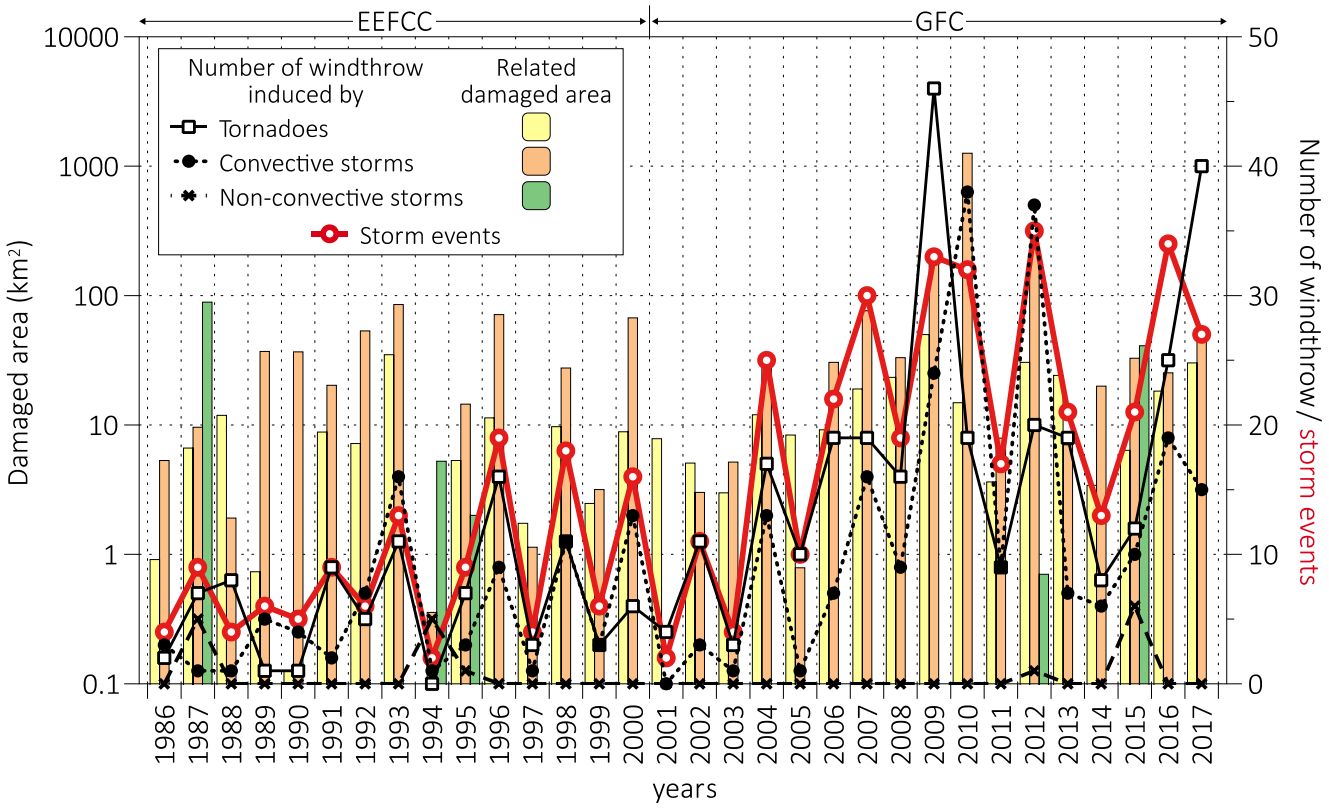

Figure ~~11~~12: Interannual variability of the number of ~~windthrows~~windthrow, related damaged area, and number of storm events. Note the logarithmic scale for the damaged area. Periods for the EEFCC and GFC datasets are indicated.

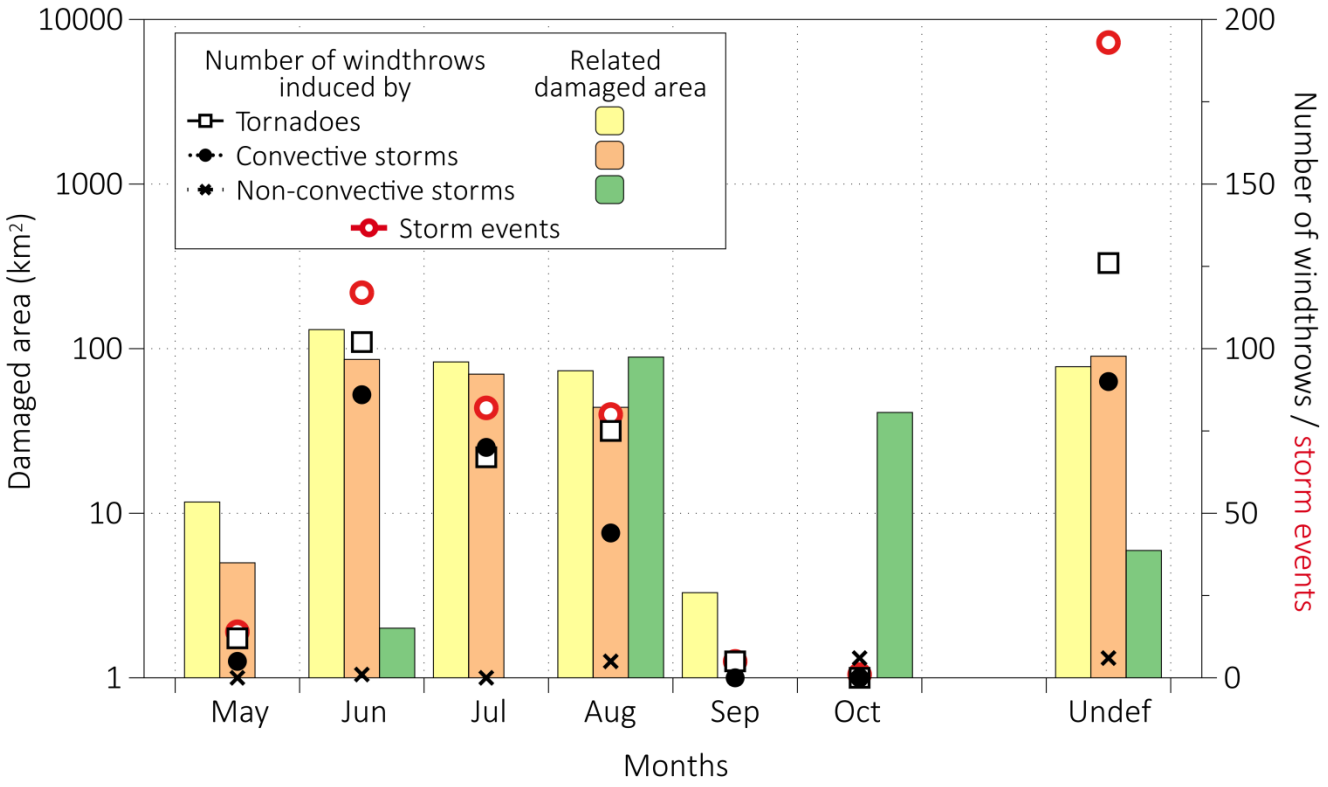

Figure ~~12~~13: Annual cycle of the number of ~~windthrows~~windthrow, related damaged area, and number of storm events. Note the logarithmic scale for damaged area.

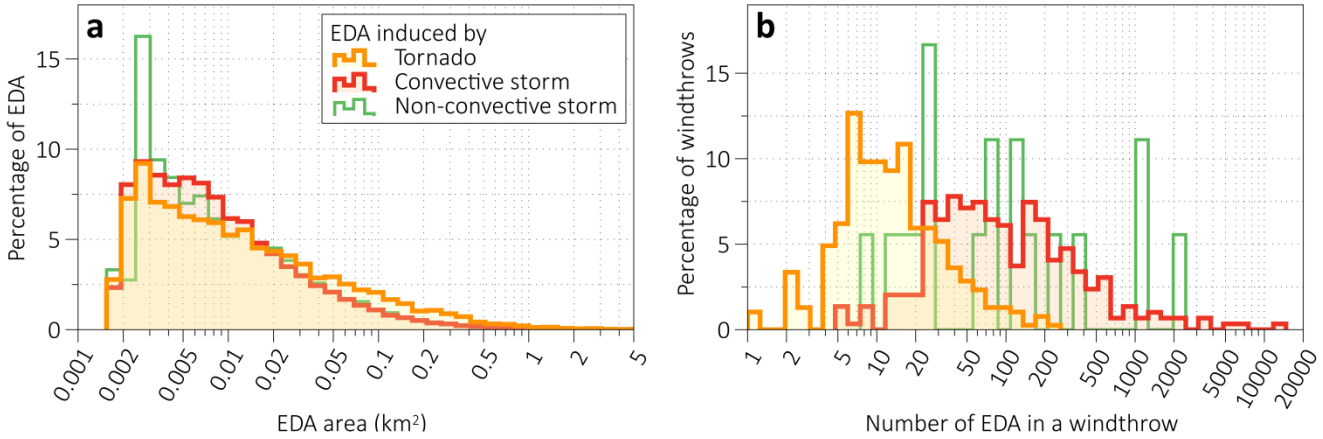

Figure ~~13~~14: Distribution of (a) size of EDAs for different types of ~~windthrows~~windthrow and of (b) a number of EDAs within one windthrow.

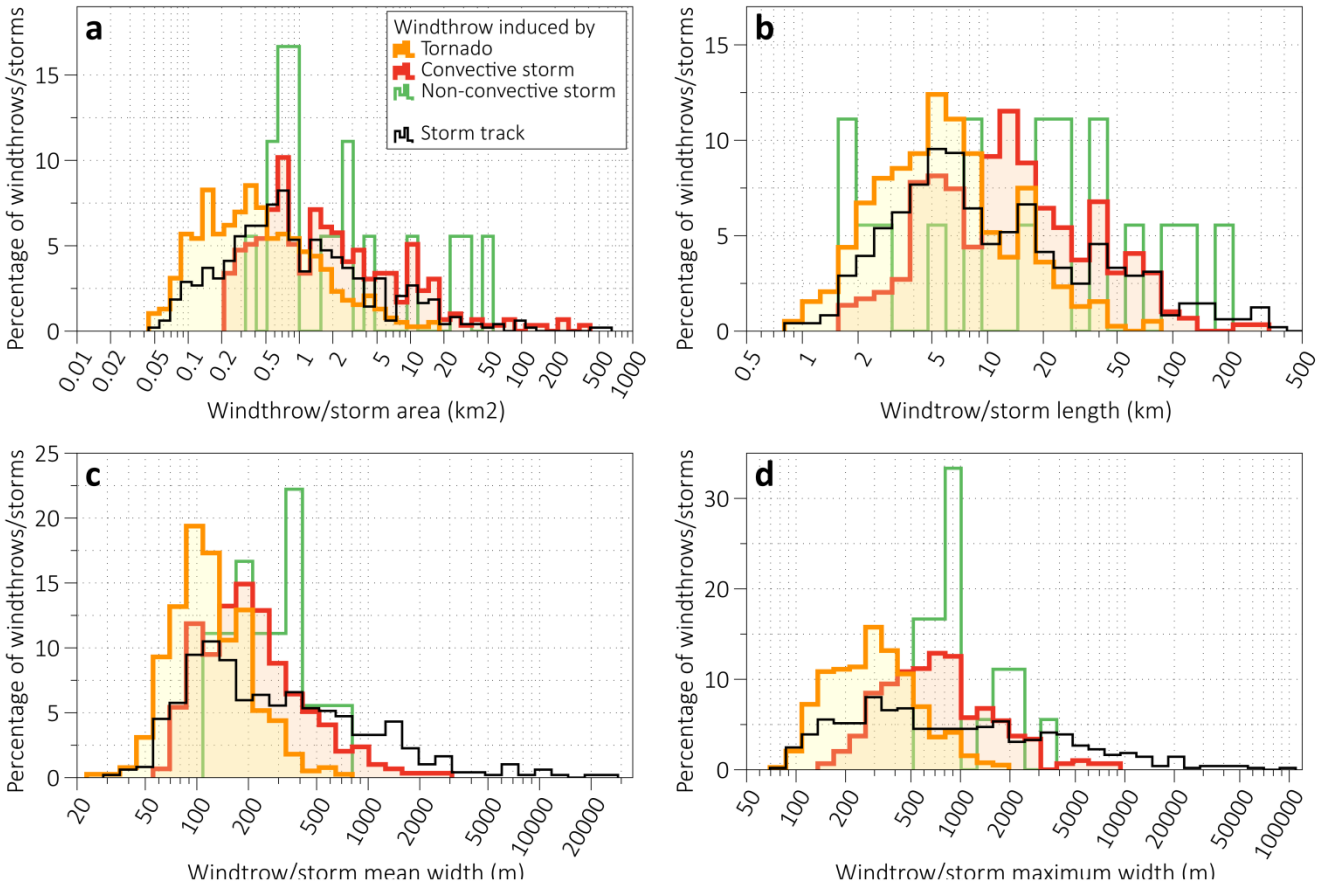

Figure ~~14~~15: Distribution of geometric parameters of ~~windthrows~~windthrow of different types and storm tracks: (a) area, (b) length, (c) mean width, and (d) maximum width.